2008

Investigation into the stress assisted damage of copper surface under single asperity: influence of contact pressures, surfaces stress states and environments

Bun Hiong Chua
Iowa State University

Investigation into the stress assisted damage of copper surface under single asperity: influence of contact pressures, surfaces stress states and environments

by

Bun Hiong Chua

A thesis submitted to the graduate faculty

in partial fulfillment of the requirements for the degree of

MASTER OF SCIENCE

Major: Mechanical Engineering

Program of Study Committee:
Abhijit Chandra, Co-major Professor
Pranav Shrotriya, Co-major Professor
Andrew Hillier

Iowa State University

Ames, Iowa

2008

DEDICATION

I would like to dedicate this thesis to my loving wife, Tina Yen, who has been very supportive throughout my life journey. I also thank God for providing my daily needs and the opportunity to further my studies. Thanks to my family and friends, who love and care about me so much. Last, but not least, my major professors and committee member for making my academic journey interesting and fruitful.

TABLE OF CONTENT

CHAPTER 1: GENERAL INTRODUCTION

1.1 Single Asperity Wear of Copper

Copper is becoming a commonly used material serving as interconnect material in advanced submicron multilevel technologies because of its high electrical conductivity and good heat resistance [1]. It is about 40% lower resistivity than aluminum and 100% lower resistivity than aluminum alloys at room temperature [2]. Moreover, copper has very high melting temperature, about 1083degree Celsius [3]. Therefore, many researches show different behaviors of copper when exposed under different conditions, for instant, mechanical delamination and chemical dissolution. In integrated circuit multilevel fabrication, it is necessary to ensure the surface planarization before the next layer is deposited. Therefore, polishing process is needed to remove the excessive material deposited. In typical polishing process, the material surface is mechanically abraded with multiple abrasives. Each abrasive contributes to the overall polishing process and leading to the global planarization. Chemical Mechanical Planarization (CMP) process has become the most promising method in producing a better local and global surface planarization. Previous works show different factors such as the speed of the process, contact loads and chemical reaction that influence the material removal during a polishing or wear process [4-6]. A brief introduction of CMP is presented in the next section.

1.2 Application: Chemical Mechanical Planarization (CMP)

Copper damascene processing has been developed to achieve copper metallization [14,15] continued by chemical mechanical planarization to remove excessive materials and

planarize the surface. CMP is needed to achieve reliable interconnection between multilayer chips that the thickness across the surface is uniform before each layer is deposited. During copper CMP processes, copper surface is undergoing mechanical abrasion and chemical reactions. The schematic of CMP is presented in figure 1. The abrasives in the slurry such as alumina and silica abrade the surface of the material and the process is assisted by the chemical reaction.

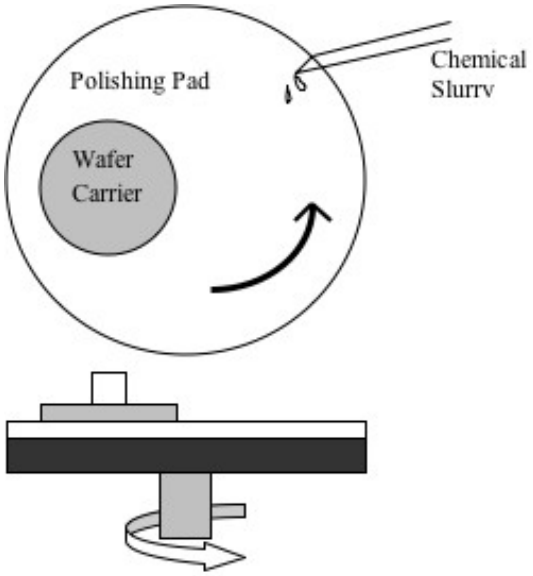

Figure 1 Schematic of Chemical Mechanical Planarization process consisting wafer carrier, polishing pad and chemical slurry.

The process of mechanical polishing usually follows an empirical theory, Preston formula wherein the material removal rate is given by:

$$MRR = K.P.V \qquad (1)$$

where K is the Preston proportionality constant based on chemical effects, P is the applied down pressure and V is the relative velocity of wafer [17]. However, Preston's equation only

reflects the influence of applied down pressure and velocity. Many experiments has shown effect of other different factors on the material removal such as the material of the polishing pad, the surface stress state, slurry composed of nano-scale abrasives and the hardness of the polishing pad and material [18-21]. The hardness of the material surface is affected by the grain size of the material where smaller grain size increases the hardness of the material [26].

Firstly, the contact pressure plays a very important role in CMP processes. There are two typical contact modes during CMP, namely the hydrodynamic contact mode and solid-solid contact mode [6], which is determined by the applied contact pressure. In the hydrodynamic contact mode, the wafer has no contact with the polishing pad leaving the abrasives in the slurry slowly remove the material whereas in solid-solid contact mode, the wafer is pressed against the polishing pad leading to a high material removal. It was shown that the surface roughness and properties of the wafer and polishing pad greatly influences the number of active abrasives [5-7].

Meanwhile, the process is assisted by the chemical reaction. The pH of the chemical has great effects on the chemical reaction. Other than the chemical itself, when a surface is stressed, the troughs of the surface experience the maximum surface stress (compressive or tensile) and greatly influence the mechanical stimulation and chemical reaction. Therefore, it is important to study both the surface delamination and chemical dissolution in different environments with different contact loads and surface stress states. The chemicals chosen for this study is discussed in the next paragraph.

1.3 Chemical Environments Investigated

Pourbaix diagram of copper is used to determine the chemical being used in this study. In the solution with different pH, copper counters different chemical reaction namely corrosion or passivation [22]. The Pourbaix diagram is presented in figure (2). For acidic (<pH7) chemical environment, copper experiences corrosion process and the material is etched continuously. In alkaline solution (>pH7), oxide layer will form on the surface of the material called passivation process. It is very interesting to be able to compare the differences when the experiment is performed in different chemical reaction processes. In order to do that, three solutions were chosen to represent each process: corrosion, passivation and solution in between. The pH of chemical is measured before and after the experiment to monitor any possible pH changes.

De-ionized water is used to demonstrate the process in between corrosion and passivation. The pH of pure water was supposed to be around pH of 7, but when water is exposed to the atmosphere, it reacts with carbon dioxide in the air and forms carbonic acid. Therefore, the measured pH of de-ionized water is around 6, which will follow the manner of corrosive solutions.

One of the commonly used passivation solution is ammonium hydroxide [23-24]. The pH of the solution used in the present investigation is about 9. When the material is exposed to the solution, an oxide film is formed on the surface of the surface. The material encounters rapid passivation when the oxide layer is mechanically removed.

Nitric acid is one of the widely used acidic chemicals with copper due to the strong etching reaction. Copper oxide layer is removed from the surface and copper is dissolved in the solution. In order to prevent the material from being totally dissolved into the solution,

corrosive inhibitor is used. Many researches have shown promising ability of benzotriazole (BTA) to react with copper to form Cu-BTA layer on the surface [23-25]. The thin film will serve as the oxide layer and guarding the surface from rapidly corroded by the solution and fulfilled the required condition of rapid passivation during CMP processes [13].

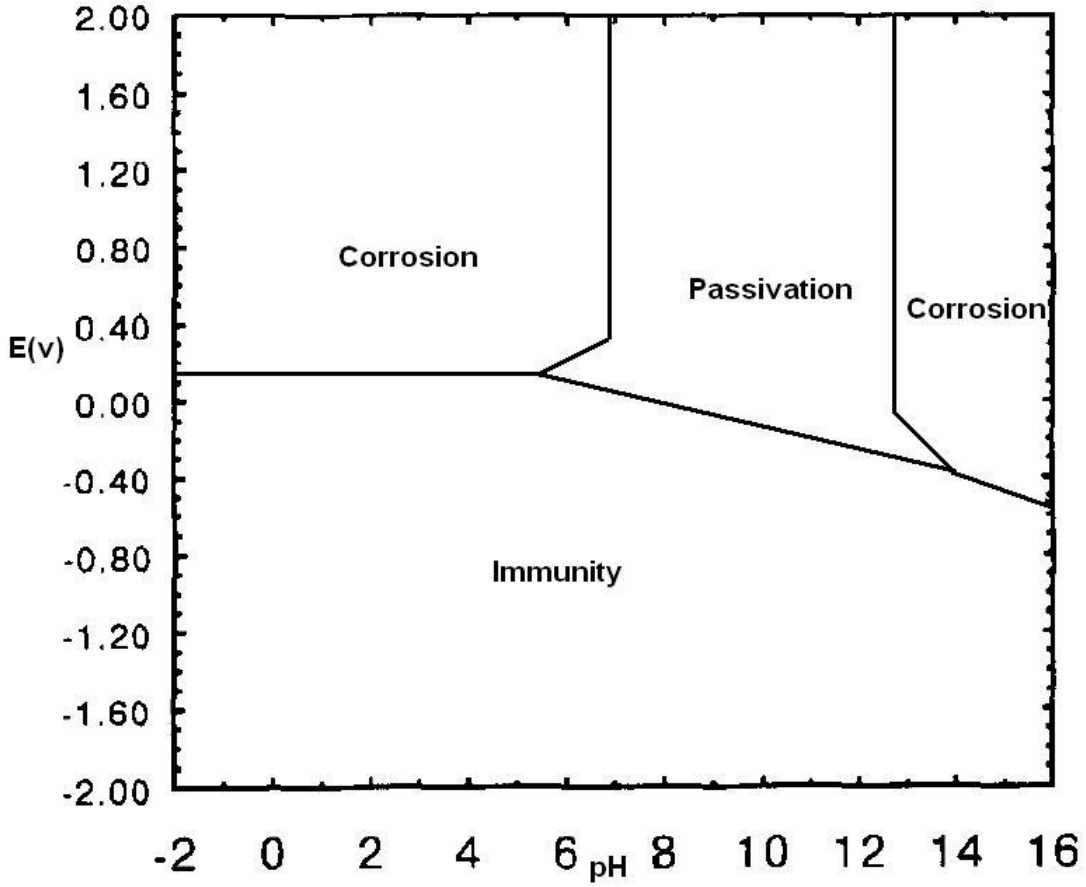

Figure 2 Pourbaix diagram of copper showing different surface condition in different environment.

1.4 Research Objective

The primary objective of this research is to investigate the mechanism of material removal of copper under single asperity in terms of contact pressures, surface stress states and environments. Because of copper is gaining more and more interests in integrated circuit device manufacturing, many advanced technologies have been developed to ensure reliable fabrication. Many previous researches have been done to investigate the main effects of material removal during copper polishing/wear but a mechanism based understanding of the synergistic interactions between chemical environment and mechanical loading is still lacking. Moreover, the surface roughness plays a very important role in copper polishing, which surface stresses are generated according to the surface roughness when a force is normally applied against the surface. The maximum compressive or tensile stresses in a specific region tend to appear at the trough of the surface when a normal force is applied to the peaks. Therefore, this research utilizes a four point bending setup to generate a range of surface stresses from compressive to tensile stress to model the phenomena. An Atomic Force Microscopy (AFM) cantilever is used to serve as a single asperity wear of the polishing process. Various contact pressures are used to study the influence of abrasives diameter and forces during a bulk abrasives polishing. The chemicals used in this research are intentionally modeling the process in different reaction processes whether it is corrosion or passivation. The chemical reaction rate due to the surface stress state is also one of the main focuses in the present study. It is hoped that the data obtained in this research will be a contribution to the wear model during material nano-scale polishing.

1.5 Thesis Outline

In order to better explain the investigation, this thesis consists of five chapters. A brief introduction and research objective are discussed in the current chapter followed by a chapter illustrating experiment design such as four point bending frame and equipment calibrations. Chapter 3 and 4 are presented as papers to be submitted for publications. They consist of abstract, introduction, experiment setup, results, discussion and conclusion. A general final conclusion of this thesis is included in Chapter 5.

Results of the experiment performed in ambient condition are included in Chapter 3. The objective of the experiment is to study the influence of contact loads and surface stress states on material removal of copper on a single asperity wear without any chemical reaction and the sample is reacting with the atmosphere. Detailed analyses such as contact load with adhesive force and possible error are presented and discussed.

For further investigation, the experiment was performed in various aqueous conditions. The experiment setup will be presented in Chapter 4. The results obtained will be compared according to the different chemical reactions in addition to the influence of contact loads and surface stress states. Details of the experiment such as the experiment setup, error and contact pressure analysis will be presented. The material removal mechanism based on mechanical stimulation and chemical dissolution will be discussed and compared to previous works.

CHAPTER 2: EXPERIMENTAL SETUP DESIGN

2.1 Experiment Fixture Design and Calibration

The purpose of the fixture is to generate a range of both compressive and tensile surface stresses on the sample surface regardless of the sample material properties. Besides, the design has to be adjustable to accommodate different sample geometries and apply a stress level below the yield strength of the sample. The fixture must be reusable for multiple tests- high yield strength for the fixture material so the fixture only encounters elastic deformation during sample loading and unloading. The applied load needs to be adjustable depending on the type of material used for testing. The design needs to be placed under AFM and constrain the total thickness of the frame to be under the total distance between the AFM piezoelectric and the stage, which is about an inch. The details of the setup and theory behind it will be discussed in the next paragraph.

The experiment setup was designed based on the previous similar work done on cobalt chromium [20-21]. The experiment setup consists of five major elements: a C-clamp, base with extrusion, four rollers, capacitance gage and sample. The schematic of the design is presented in figure 2. The total height of the sample and rollers has to be greater than the distance between the bottom of the C-clamp and extrusion. When the sample and rollers are placed in-between the c-clamp and extrusion of the base, they force the C-clamp to open. As a result, a force, P, is distributed across the four rollers from the C-clamp to the sample. The rollers at the bottom of the sample are separated by a distance of one inch and the rollers at the top are separated by one half inch. This allows sufficient sample surface area to be tested, which is the area between the two rollers at the top. The sample geometries must be well

designed where the thickness has to be less than the thickness of the C-clamp in order to prevent external force applied on the sample. The free-end deflection of the C-clamp is monitored by a capacitance gage attached to the C-clamp. The gage measures the air gap between the end of the c-clamp and sensor to measure the capacitive reactance. It acts like a parallel plate capacitor in a DC circuit. The resistance/distance between the plates is used to determine the loads applied to the sample. Greater resistance indicates larger distance, hence, larger load. A schematic of the setup is shown in figure (3).

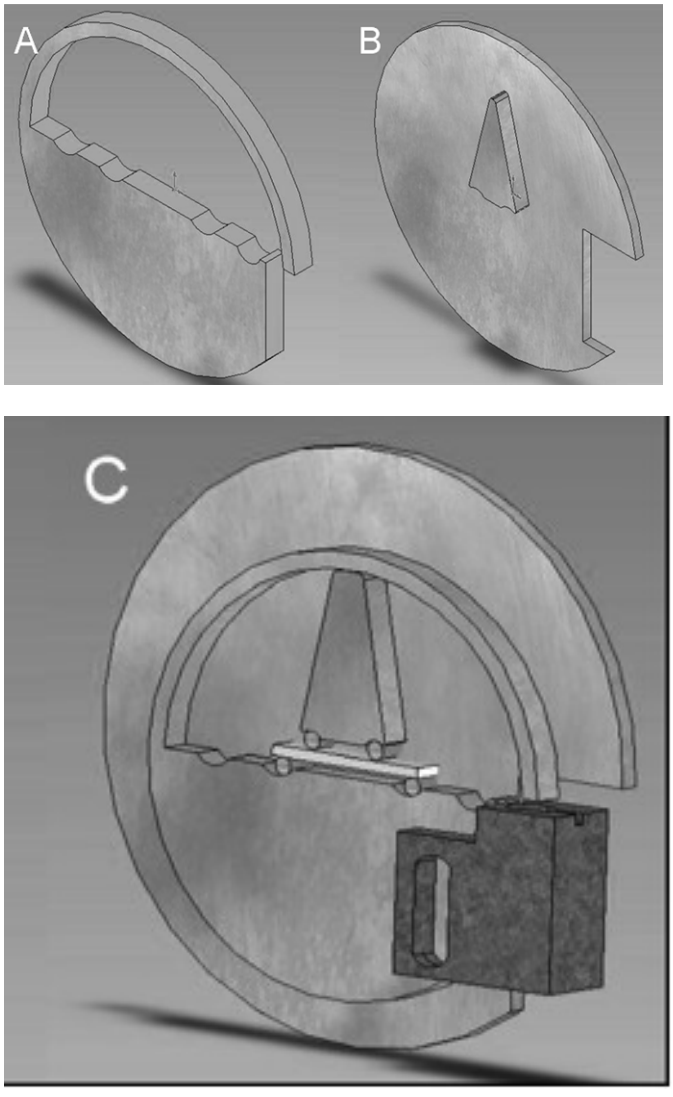

Figure 3 A complete setup for generating a various surface stress state. It consists of base, C-clamp, capacitance gage, four rollers and rectangular sample. (A) C-Clamp, (B) Base with extrusion.

The capacitance gage used in this application is very important. It determines the actual surface stress applied by the C-clamp. When considering the gage to be used, the size is one of the biggest factors since the thickness of the gage need to be equal or smaller than the total thickness of base plus C-clamp in order to allow the setup to lie down horizontally. Other major factors are the gage has be a non-contact sensor due to this particular application and the ease of use. Electrical capacitance gage seems to be the best fit since it only requires minimum additional equipment and skills. In order to limit the C-clamp deflection to only elastic deformation, the free-end deflection is limited to 1mm (factor of safety of 2). This value varies according to the material properties and geometries of the C-clamp. To accommodate this limit, the gage chosen serves as a secondary safety device for the design by warning the user if the deflection exceeds 1mm. After considering all the requirements above, the specific gage decided was the Capacitec HBP-75 with a linear range of a little over 1mm.

To determine the amount of load experienced for the C-clamp, it was calibrated by a dead weight method. By calibrating the C-clamp, the relationship of load and free-end deflection can be obtained. Calibration weights were applied to the top of the C-clamp. The deflection was monitored and recorded. The process is repeated with different load with 0.1lb increments until deflection slightly below 1mm was reached. The deflection is plotted against calibration load to quantify the relationship between them. It is show in figure (4). The unit was converted into SI unit system. The relationship is determined as:

$$P = 0.024\,\delta \qquad (2)$$

where P is the load applied to the sample in Newtons and δ is the free-end deflection in microns.

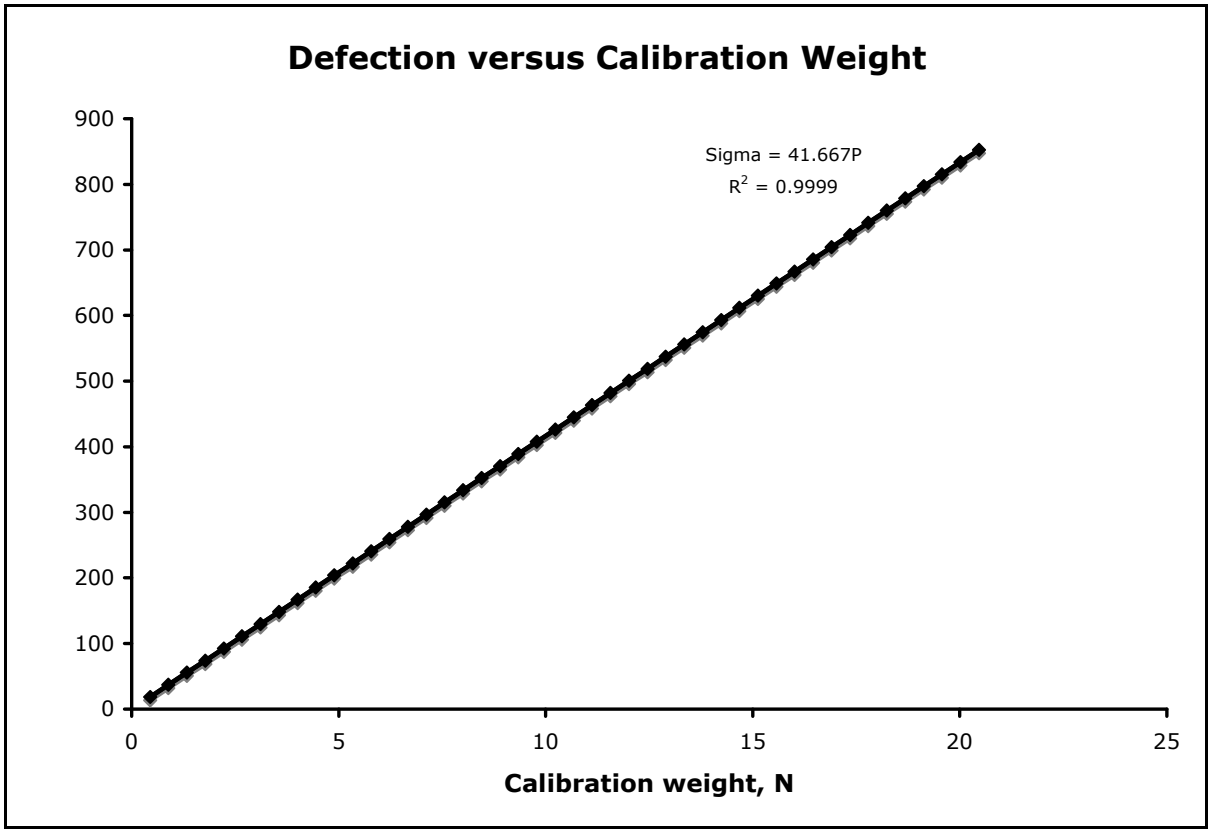

Figure 4 Graph showing the C-clamp free end deflection plotted against calibration weight.

After the C-clamp was calibrated, the next step is to identify the load required to generate desired surface stresses. The surface stress calculation is according to the sample's height and width (cross sectional area) along the sample. Required deflection was calculated based on the desired applied load needed. The sample geometries are fixed and the required deflection is achieved by varying the size of rollers. The rollers used in this experiment must be able to withstand the maximum load applied from the C-clamp without experiencing deformation. Therefore, the rollers chosen were heat-treated 52100 bearing steel gages (modified pin gages from Meyer's Gage Company, South Windsor, CT). The theory and analysis of this study will be discussed in the next section.

2.2 Theory

As discussed above, the surface stress applied by the four-point-bending design can be determined without knowing the physical properties of the materials. In order to find the applied stress across the rectangular sample, the following equation is needed:

$$\sigma = Mc/I \qquad (3)$$

where σ is the applied stress, M is the constant moment, c is the distance between the desired location and the neutral axis and I is the second moment of inertia. c and I are known according to the sample's cross sectional area as shown in figure (5):

$$c = h/2 \qquad (4)$$

$$I = bh^3/12 \qquad (5)$$

where b and h are the width and height of the cross sectional area of the sample respectively. Once the sample is loaded, the only unknown in the equation is the moment, M which will be discussed in the next section.

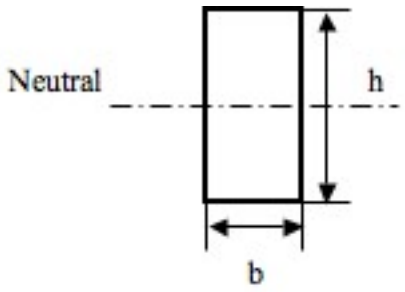

Figure 5 schematic showing the cross sectional area of the sample

As shown in figure (7) the moment can be calculated according to the sample's length and applied force. The moment of the area between the rollers at the top can be defined as:

$$M = PL/8 \qquad (6)$$

where M is the moment, P is the applied force and L is the length of the sample, in this case a fixed value of 25mm. After the sample and rollers are placed between the C-clamp and base extrusion, the free end deflection of the C-clamp is recorded and used to measure the actual load applied to the sample, P. Hence, the moment can be calculated. Plug in all the parameters found into equation (3) to calculate the stress applied. A wide range of surface stresses from compressive to tensile stress is achieved at the top and the bottom of the sample respectively.

In order to determine the stress at a specific location, a high-resolution camera is used to identify the surface features such as scratched and impurities which serve as reference points around the desired location prior each experiment. The distances of the reference points away from the edges are calculated. Figure (6) shows the possible location to be scanned with various contact load and surface stress states. When the experiment setup is placed under AFM, the defects are located and recorded with the AFM camera. The cameras magnification ratio is obtained and being reuse in the analysis of other samples.

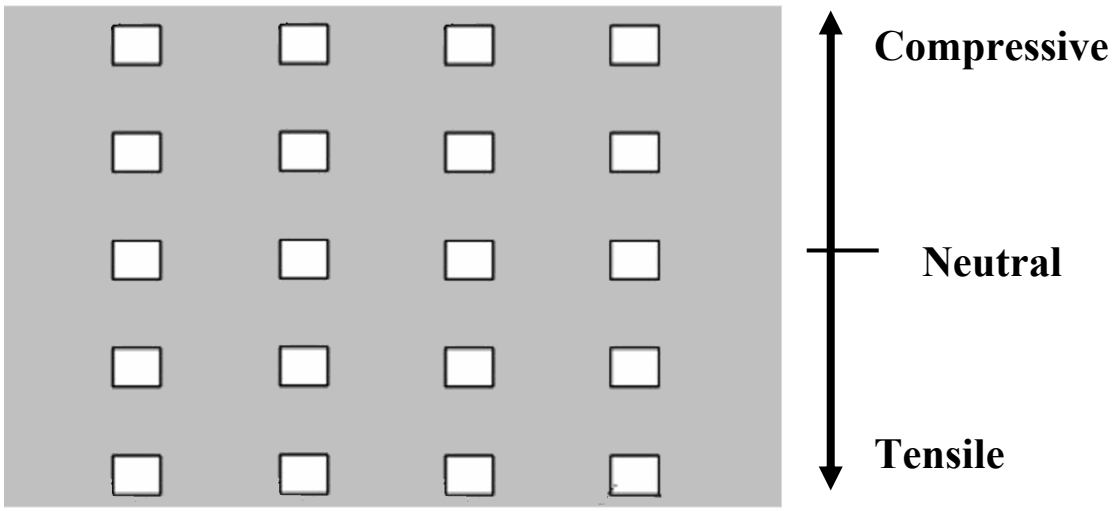

Figure 6 Compressive are applied at the top of the sample and tensile stress at the bottom of the sample.

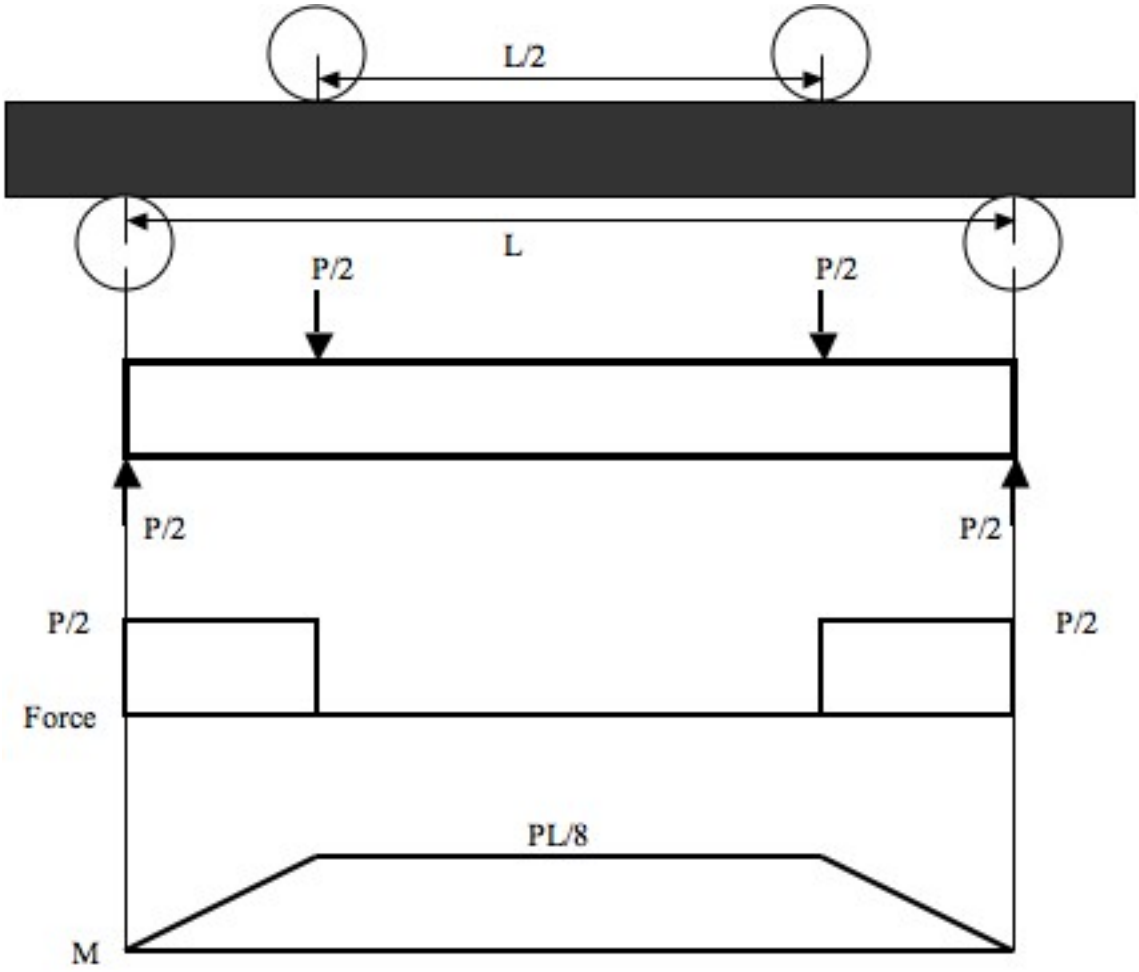

Figure 7 Shear force and moment diagram of a rectangular sample in four point bending. The constant moment is developed in-between the two rollers on the top of the sample.

2.3 Reference

[1] Ein-Eli, Y., Abelev, E., Rabkin, E. and Starosvetsky, D., "The Compatibility of Copper CMP Slurries with CMP Requirements." *Journal of The Electrochemical Society*, 150 (9) C646-C652, 2003.

[2] *CRC Handbook of Chemistry and Physics,* CRC Press, Boca Raton, FL

[3] Murarka, S.P., *Metallization,* Butterworth-Heinemann, Boston, 1993, p. 100.

[4] Wolf, B. and Paufler, p., "Speed Dependency of Abrasion during AFM-Scanning Under High Load", *Crystal Research and Technology,* Vol. 31, Issue 4, p. 505-511.

[5] Ando, Y., "Relationship between friction and plastic deformation examined by using periodic asperity arrays fabricated on an AFM multipurpose cantilever." *Tribology Letters,* Vol. 15, No. 2, 2003.

[6] Luo, J and Dornfeld, A., "Material Removal Mechanism in Chemical Mechanical Polishing: Theory and Modeling." *IEEE Trans. On Semiconductor Manufacturing,* Vol. 14, No. 2, 2001

[7] Nishioka, T., Sekine, K., and Tateyama, Y. "Modeling on hydrodynamic effects of pad surface roughness in CMP process." *Interconnect Technology, 1999, IEEE International Conference,* p. 89-91, 1999

[8] Che, W, Bastawros, A. and Chandra, A., "Surface Evolution during the Chemical Mechanical Planarization of Copper." *CIRP Annals- Manufacturing*, Vol 55/1, P. 605-608, 2006.

[9] Yu, H.H., Suo, Z., "Stress-dependent Surface Reactions and Implications for a Stress Measurement Technique," *Journal of Applied Physics*, Vol. 87, Issue 3, p. 1211-1218, 2000.

[10] Kim, K. S., Hurtado, J. A. and Tan, H., "Evolution of a surface-roughness spectrum caused by stress in nanometer-scale chemical etching." *Physical Review Letter*, 83: P. 3872-3875, 1999.

[11] Carpio, R., Farkas, J. and Jairath, R., "Initial Study on Copper CMP Slurry Chemistries." *Thin Firm*, 266, p. 238-244, 1995.

[12] Luo, Q., Campbell, D.R. and Babu, S.V., "Chemical –Mechanical Polishing of Copper in Alkaline Media*," Thin Solid Films*, 311, p. 177-182, 1997.

[13] Kaufman, F. B., Thompson, D. B., Broadie, R. E. and Jaso, M. A. "Chemical-Mechanical Polishing for Fabricating Patterned W Metal Features as Chip Interconnects." *Journal of Electrochemical Society*, Vol. 138, 3460, 1991.

[14] Sethuraman, A.S., Wang, J.F. and Cook, L.M., "Review of planarization and reliability aspects of future interconnect materials*" Journal of Electronic Materials*, Vol. 25, No. 10, 1996.

[15] Jindal, A. and Babu, S.V., "Effect of pH on CMP of Copper and Tantalum", *Journal of The Electrochemical Society*, 151 (10) G709-G716, 2004.

[16] Dejule, R., "CMP challenges below a quarter micron." *Semicond. Int.*. p. 54-60, 1997.

[17] Preston, F.W., *The theory and design of plate glass polishing machine*, J. Soc. Glass Technol., 1927, 11, No44, p. 214-256.

[18] Xu, R. Smart, G and Chang, M., "Particle characteristics and removal rate in CMP process." Proc. Fourth Int. Chemical-Mechanical Planarization for ULSI multilevel Interconnection Cond., Santa Clara, CA, Feb 11-12. P. 253-255, 1999

[19] Pohl, M. C. and Griffiths, D. A., "The importance of particle size to the performance of abrasive particles in the CMP process." *Journal of Electronic Materials*, Vol. 25, p. 1612-1616, 1996.

[20] Mitchell, A., Shrotriya, P., "Onset of nanoscale wear of metallic implant materials: Influence of surface residual stresses and contact loads." *Wear***,** Vol. 263, Iss. 7-12, 2007, P. 1117-1123

[21] Mitchell, A. and Shrotriya, P. " Investigation into the onset of nanoscale surface damage of biomedical grade CoCrMo: Influence of contact loads, residual stresses, and environment," Master's Thesis, Iowa State University, 2005.

[22] Pourbaix, M., *Atlas of Electrochemical Equilibria in Aqueous Solution*, Pergamon Press, Cebelcor Brussels, 1966. p. 384-392.

[23] Steigerwald, S.P. Murarka, R.J., Gutmann, D.J. Duquette, "Chemical Processes in the Chemical Mechanical Polishing of Copper." *Meterial Chemistry and Physics*, 41, p. 217-228, 1995.

[24] Luo, Q, Mackay, R. A. and Babu, S. W., "Copper Dissolution in Aqueous Ammonia-Containing Media during Chemical Mechanical Polishing." *Chemistry of Material*, Vol. 9, p. 2101, 1997.

[25] Luo, Q., Campbell, D.R. and Babu, S.V., "Stabilization of Alumina Slurry for Chemical-Mechanical Polishing of Copper." *Langmuir*, Vol. 12, p. 3563-3566, 1996.

[26] Correia, J.B., Marques, M.T., Carvalho, P.A. and Vilar, R., "Hardening in copper-based nanocomposites", *Journal of Alloys and Compounds,* Vol. 434-435, p. 301-303, 2007

CHAPTER 3: SINGLE ASPERITY WEAR OF COPPER: INFLUENCE OF SURFACE STRESS STATE

A paper to be submitted to Wear

Bun-Hiong Chua, Pranav Shrotriya and Abhijit Chandra
Department of Mechanical Engineering, Iowa State University, Ames, Iowa 50011, USA

3.1 Abstract

Nano scale wear response of copper was investigated as a function of contact loads and surface environment. An experiment setup was used to generate a range of surface stress state on a well-polished copper sample. A single asperity contact was modeled using the cantilever tip of an Atomic Force Microscope (AFM). Different contact pressures applied on the sample were determined by measuring the loads applied and the radius of the cantilever. Controlled tip contact pressures were applied on the copper surface to mechanically stimulate the stressed surface. The processes were performed in ambient condition with relative humidity of 30-40% and material removal was measured as a function of contact pressure and surface stress state. The results show the material removal rate was higher with higher contact pressures, but with constant pressure, the rate increased significantly in the compressive surface stress compared to tensile stress. A mechanism of the surface damage based on stress-assisted delamination was developed to explain the experiment results.

3.2 Introduction

Copper is one of the most ideal materials used in semiconductor manufacturing. Since copper has very low resistivity and high melting temperature, it provides good electromigration resistance [1]. As the popularity of copper increases, many experiments have been undertaken to investigate its behavior in different processes such as deposition, etching and polishing processes. One of the most important processes in integrated circuit devices manufacturing is the metal interconnection forming process. Copper based devices are manufactured using additive patterning continued by polishing processes to remove excessive material to provide good surface planarization. This is needed before the next layer is deposited onto the surface to ensure reliable interconnections. Currently, chemical mechanical planarization (CMP) is the most promising polishing methods in IC manufacturing, which utilizes both chemical reaction and mechanical abrasion to achieve global planarization. During CMP, the abrasives in the slurry mechanically stimulate the surface along with chemical reactions that softens or corrodes the material at the same time. One mostly used equation to determine the material removal rate of the process is Preston equation, which shows the material removal is affected by three elements: chemical reaction, applied pressure and relative velocity [2].

The focus of the current study is the mechanical abrasion process of a single particle without the present of chemical reactions through performing the experiments in ambient condition. The actual contact pressure of the particles and surface is determined by the particle size and force applied to the surface. The absorption of water on the material surface increases the contact force by the amount of adhesive force. Therefore, as many authors have shown, sliding wear in dry condition causes high friction force between the surface and

particle resulting higher material removal rate compared to in aqueous conditions. This phenomenon is similar to the wear mechanism in many kinds of process such as the fretting contact in medical devices, turbine blade and ball bearings where the surface damage is affected by the amount of contact pressure. In this specific case, the required shear stress to nucleate dislocations in copper is about 1.6Gpa [8]. However, the number varies based on the method the material is produced and the environment conditions.

Other than the contact pressure and speed, surface delamination is also affected by surface stress state [9]. Researches performed on cobalt chromium shows that the surface experiences reactions with the atmosphere and form an oxide layer on the surface of the material. While the oxide layer is removed from the surface, repassivation takes place and another oxide layer is form [3,10]. The material removal rate is accelerated by the compressive stress and suppressed by the tensile stress. In the same manner, copper reacts with the oxygen in the air and form copper oxide layer on the surface. In the current study, the oxide layer is mechanically stimulated and removed followed by repassivation process to form another oxide layer. The surface delamination and repassivation process is either accelerated or suppressed by a stressed surface.

In the current study, we will focus on the mechanism of mechanical abrasion of copper wear under single asperity. Although many have shown the material removal rate is greatly influenced by the applied contact pressure related to the particle size and polishing speed [4], a mechanism based understanding of other factors such as either pre-existing or applied surface stress state effect is still lacking. The synergistic interactions between surface stress state and material removal is investigated in the current study. The advanced technology of atomic force microscope (AFM) makes investigation the mechanisms of wear

possible in small scale and light load [5]. Many other previous works have been undertaken in order to investigate the unique behaviors of different materials under single point indentation or scratch. Many of these experiments are done in dry condition in order to study every single possible factors of wear process such as the surface coefficient of friction during the sliding process using an AFM tip [5-7]. In this case, we utilize an AFM cantilever probe to model the single asperity wear of copper surface with different applied contact pressures. In order to demonstrate the effect of various surface stresses, a four-point-bending setup is used to generate a stress range from compressive through tensile across the sample. The material removal results of copper wear under various contact pressures and surface stress states will be presented and discussed. The experiment setup and procedures will be discussed in the next section.

3.3 Sample Preparation

Material used in this investigation is 99.9% copper. A 2.5mm copper plate was cut into several rectangular bars (1.25mm x 2.5mm x 25mm) for being put under the experiment in ambient conditions. Mechanical properties of copper used are presented in table 1. One side of the sample surfaces (area of 1.25mm x 25mm) were mechanically polished first by using 600 grit with water, then with 3μm diamond suspension with lapping oil on nylon pad and finally with 0.05μm alumina suspension with de-ionized water on Microcloth. The sample was polished until mirror-like surface was obtained. Due to the softness of copper, achieving a scratch-free is impossible. Therefore, initial AFM scan of the surface was used to study the surface topography and roughness. The surface root mean square (RMS) roughness of the sample was maintained to be 4nm to 6nm.

Several copper samples were etched with 1g FeCl3, 10mL HCl and 100mL water [17] to determine the average grain size. The microstructure is presented in Figure (1) and reveal large grain size, in this case approximately 25micron.

3.4 Four Point Bending Frame

A unique four-point bending setup was used in this study. The setup consists of four elements: the base, C-clamp, a capacitance gage (Capacitec, Myer, MA) and four rollers (modified pin gages from Meyer's Gage Company, South Windsor, CT). The setup is schematically shown in figure (2). Various surface stress states were generated across the polished copper surface with the setup. The C-clamp was calibrated by using dead weight method to determine the deflection as a function of load. When the rollers and sample were place between the C-clamp and extrusion on the base, they force the C-clamp to open against the base. The force applied was determined by monitoring the C-clamp free-end deflection. The relationship between the load and deflection for the C-clamp used is

$$P = 0.024\delta$$

where P is the applied force (Newtons) generated through the C-clamp and δ is the deflection (microns). After the fixture was setup, the force applied can be calculated according to the deflection. Surface stress can be determined by measuring the sample size. Compressive stress was generated at the top of the sample surface and tensile stress at the bottom. In this study, the maximum stress on either compressive or tensile side is 70% of copper's yield strength, which is approximately 49Mpa .The location and surface stress distribution is presented in figure (3). The actual stress on any location may be determined by knowing the distance from the neutral axis.

3.5 Atomic Force Microscope (AFM) Setup and Tip Characterization

AFM probe was used to model a single asperity contact of the wear process. The specimen surface was mechanically stimulated using a Dimension 3100 atomic force microscope (AFM) with Nanoscope IV controller (VEECO Instruments, Woodbury, NY). Silicon nitride (Si_3N_4) cantilevers with a reflective gold backside coating (DNP-S VEECO Instruments, Woodbury, NY), nominal spring constant of 0.58 N/m and nominal tip radius of 30 nm were used in this study. In order to accurately determine the force to be applied through the AFM, each cantilever was calibrated before the test. Sensitivity was recorded for each run. The stiffness of the cantilever was determined by monitoring its deflection against a hard surface (sapphire), as well as against a reference cantilever with known stiffness of 0.366 N/m. The stiffness of the cantilever is found by the equation:

$$k_{cantilever} = \frac{(\delta_{SiC} - \delta_{RC})}{\delta_{RC}} * (k_{RC})$$

where 'δ' is cantilever deflection and subscript '*RC*' refers to the reference cantilever. The cantilever tip was characterized by the inverse image of scanning over a silicon spike sample with radii curvature less than 10nm. Tip radius was measured before and after each wear run to know the probe wear. The contact pressure can be calculated based on the actual force applied by the AFM tip and the tip radius.

3.6 Experimental Procedures

The setup is placed under AFM at four contact pressures and five different surface stress states. The copper sample was placed in-between the C-clamp and the base extrusion. Compressive stress state was generated at the top of the sample surface where tensile stress

state at the bottom of the sample. Then, the locations to be scanned were defined by identifying the surface features and defects on the sample. The five surface stress states are strong compressive stress, weak compressive stress, neutral, weak tensile stress and strong tensile stress states. These surface stress states were determined by measuring the distance between the scan area and the neutral axis. Before each set of data was obtained, the relative humidity of the environment was recorded. All the ambient condition experiments were performed under relative humidity of 30%-40%. The AFM was warmed up for about one hour or till no noticeable drift was observed on multiple scans due to the drifting problem of AFM. After that, it was very important to record the force curve of each experiment in order to monitor the adhesive force between tip probe and sample surface. An initial 5μm X 5μm surface topography was recorded at a contact load of 1-2nN and speed of 2Hz. After the initial topographical image was recorded, the wear tests were performed on a 2 μm X 0.5 μm window right on the center of the initial scan window. The wear process was performed with desired contact load at a speed of 5Hz for 15 minutes. After 15 minutes, the setup was reset to the initial parameters (1-2nN, 2Hz and 5μm X 5μm scan size). Final image was then recorded. The desired contact loads for the wear process were 15nN, 30nN, 45nN and 60nN. These loads were then converted into contact pressures based on the radius of the cantilever probes. The material removal rate was highly affected by the contact pressure instead of contact load because each tip has its unique shape and different radius. With a constant contact load, the contact area between tip probe and sample surface increases when the tip radius increases. Higher contact pressure was generated by sharper tip compared to the blunted (larger radius) tip. Moreover, it was necessary to measure the cantilever tip radius before and after each run to monitor the probe wear rate during the mechanical stimulation.

In order to generate a wide range of contact pressure during the scratching process, a single AFM tip was needed for each applied load. The pressures were then grouped into two to three ranges.

3.7 Data Analysis

3.7.1 Wear Rate Analysis

The material removal rate for the wear was analyzed. The initial AFM image shows the polished copper sample surface. Although it was intentionally to get a scratch free surface, but due to the material used was very soft and it was almost impossible to achieve by mechanical polishing process. The initial image was subtracted from the final image to eliminate the effects from the surface imperfections. The initial and final 5μm X 5μm AFM images are shown in figure (6). Since the drifting problem was unavoidable, the final image was registered to match the initial image by identifying the surface features on both initial and final images before the subtraction. After the subtraction, the scratched 2μm X 0.5μm areas was clearly shown on the subtracted image. The material removal rate can be found by measuring the depth of the area. The subtracted image was processed to find the average heights of the scratched and unscratched areas. The material removed was calculated with multiplying the area (2μm X 0.5μm) by the height difference between the scratched and unscratched areas. A three-dimensional image of the subtracted image highlighting the wear area is shown in figure (7). The errors of the data were estimated based on the standard deviation of four different measurements.

3.7.2 Contact Pressure Estimation

During the wear process, the contact stress between the tip and the sample surface is a function of normal and tangential loads. In order to simplify the experiment and get better comparisons of different contact loads, Hertzian analysis was used to estimate the average contact pressure. The applied contact loads were converted into contact pressure based on the tip radius. The Young's modulus and Poisson's ratio of copper and AFM tip were taken as 130Gpa/ 0.33 and 310Gpa/ 0.33 respectively [16,17]. The yield strength of copper used in this analysis is 70Mpa. The images showing the tip scanning on tip characterizer TGT01 were analyzed to determine the tip radius and wear. An example of a tip probe's AFM image before and after the wear process is shown in figure (4). It is clearly shown that the tip became blunted after the wear. The tip radius change is very significant especially in high contact loads such as 45nN and 60nN. Other than the effect of tip radius, the contact pressure is also affected by the environment conditions such as temperature and humidity. Because of the experiment was performed in ambient condition, the absorption of water on the sample surface caused an increase in adhesive force. A force curve is presented in figure (5) to demonstrate the quantification of adhesive force. It was observed that the adhesive forces were different between one another depending on the scan location and different relative humidity of the day of the experiment was performed. Higher adhesive force seemed to appear at high relative humidity. The adhesive force was added to the AFM applied force in the analysis of contact pressure.

3.8 Results and Discussions

All the experiment results are taken under ambient condition of relative humidity of 30%-40%. The adhesive force was added to the total amount of applied contact force from the AFM. It was observed that the amount of adhesive force changes at different locations causing different contact pressure even though constant force was applied by the AFM. The inconsistent loads and radius were recorded and converted to contact pressures. Since multiple cantilevers were used in the experiments, it is necessary to analyze the material removal based on the contact pressures instead of contact loads. Also, it was almost impossible to maintain a constant pressure throughout the experiment because the tip radius changes during the wear process. Therefore, contact pressures are displayed in the form of ranges.

The measured trench depths of two pressure ranges (low and high) are plotted as a function of applied surface stress state in figure (8). The error analyses of the trench depths are plus minus one standard deviation based on four different measurements. The errors of the applied surface stresses are based on the possible error of the force applied by the C-clamp and the sample thickness. As expected, the material removal rate increases when the contact pressure increases. The trench depth difference between two contact pressures within the same surface stress state is more significant on the compressive side than the tensile side of the sample. As observed, the surface was mechanically abraded even with the low contact pressure. It is consistent to the minimum required shear stress to remove material on copper is about 1.6GPa. Contact pressure around 3Gpa is sufficient to remove copper material.

The material removal of the surface is a result of two competing process - delamination and repassivation. Once the material is exposed to the atmosphere, the material

reacts with the oxygen in the air and forms an oxide layer on the surface. While the oxide layer is mechanically stimulated, the oxide layer is removed followed by rapid repassivation. Oxide layer with average thickness of 2nm is expected when exposed to the atmosphere [18]. Therefore, based on the results obtained in the present study, only the oxide layer was being removed. The process is repeated when the surface is mechanically abraded. The result obtained in this experiment shows that the material removal is affected by the surface stress state either by accelerating or suppressing the material removal process. For copper, the wear rate is linearly affected by the surface stress state where it is accelerated by compressive stress and suppressed by tensile stress. It is believe that two process are affected by the surface stress state namely the mechanical delamination and repassivation. Similar result was presented on cobalt chromium [10]. Another study shows that the repassivation reaction is affected by surface stress state where the mobility and driving force are changed [11].

It was mentioned that initial assumption of compressive surface stress state inhibit the surface damage become arguable when compared to the results obtained in the present study along with previous investigation [10]. However, a study shows that the oxides debris may improve or decrease surface damage resistance therefore depend on the loading and slip amplitude [12].

The results obtained in this investigation may provide useful information when designing a polishing process for a rough surface. When a surface is stresses, both maximum compressive and tensile stresses seem to appear at the trough of the surface. Therefore, by following the results of this experiment, stretch surface will provide higher wear resistance and compressive will accelerate the wear rate.

3.9 Conclusion

99.9% copper material removal rate during a single asperity wear process was studied as a function of contact load and surface stress state in non-reactive ambient condition. A unique fixture was used to generate various surface stress state from compressive stress at the top of the sample to the tensile stress at the bottom of the sample. Increase in contact pressure accelerates the material removal rate. For the contact pressure greater than 3Gpa, the results show the trench depth differences between contact pressures within a same surface stress state are more significant with the compressive stress than with tensile stress applied on the sample. It was also observed that, with a constant pressure, compressive stress accelerates surface damage where the tensile stress suppresses the process. It was believed that surface stress state not only influenced the repassivation process but also mechanical abrasion. A surface damage mechanism of the stress assisted delamination of native oxide covered surface and repassivation in the function of contact pressure and surface stress was discussed to explain the experiment observations.

3.10 Acknowledgements

The authors would like to thank Dr. Sriram Sundararajan and K.S.Kanaga Karuppiah for valuable discussion on the atomic force microscope experiments. This research is financially supported by Binger Research Fund and NSF Projects.

3.11 References

[1] Ein-Eli, Y., Abelev, E., Rabkin, E. and Starosvetsky, D., "The Compatibility of Copper CMP Slurries with CMP Requirements." *Journal of the Electrochemical Society*, 150 (9) C646-C652, 2003.

[2] Preston, F.W., *The theory and design of plate glass polishing machine*, J. Soc. Glass Technol., 1927, 11, No44, p. 214-256.

[3] Catelas, I., Bobyn, J. D., Medley, J. B., Krygier, J. J., Zukor, D. J. and Huk, O. L., "Size, shape and composition of wear particles from metal—metal him simulator testing: Effects of alloy and number of loading cycles," 2003.

[4] Xie, Y. and Bhushan, B., "Effect of particle size, polishing pad and contact pressure in free abrasive polishing." *Wear*, Vol. 200, No. 1, p. 281-294, 1996

[5] Bhushan, B., "Nano to microscale wear and mechanical characterization using scanning probe microscopy." *Wear*, Vol. 251, p. 1105-1123, 2001

[6] Zhao, X. and Bhushan, B., "Material Removal Mechanisms of Single-Crystal silicon on nanoscale and Ultralow Loads." *Wear*, Vol. 223, p. 66-78, 1998

[7] Bhushan, B., Gupta, B.K. and Azarian, M.H., "Nonoindentation, Microscratch, Friction and Wear Studies of Coatings for Contact Recording Aplication." *Wear,* Vol. 181-183, p. 743-758, 1995.

[8] Bahr, D.F., Vasquez, G., "Effect of solid solution impurities on dislocation nucleation during nanoindentation*," MRS*, Vol. 20, No. 8, p. 1947-1951, 2005.

[9] Wiklund, U., Gunnars, J. and Hogmark, S., "Influence of residual stresses on fracture and Delamination of Thin Hard Coating." *Wear,* Vol. 232, p. 262-269, 1999

[10] Mitchell, A., Shrotriya, P., "Onset of nanoscale wear of metallic implant materials: Influence of surface residual stresses and contact loads." *Wear***,** Vol. 263, Iss. 7-12, 2007, P. 1117-1123.

[11] Howatson, A.M., Lund, P.G. and Todd, J.D., *Engineering Tables and Data,* London; New York : Chapman and Hall, 1991.

[12] Ho, S. P., Carpick, R. W., Boland, T. and LaBerge, M. "Nanotribology of CoCr-UHMWPE TJR prosthesis using atomic force microscopy," *Wear*, vol. 253, p. 1145-1155, 2002.

[13] Yu, H.H., Suo, Z., "Stress-dependent Surface Reactions and Implications for a Stress Measurement Technique," *Journal of Applied Physics*, Vol. 87, Issue 3, p. 1211-1218, 2000.

[14] Iwabuchi, A., "The Role of Oxide Particles in the Fretting Wear of Mild-Steel." *Wear,* Vol. 253, p. 795-802, 2002.

[15] Ho, S. P., Carpick, R. W., Boland, T. and LaBerge, M. "Nanotribology of CoCr-UHMWPE TJR prosthesis using atomic force microscopy," *Wear*, vol. 253, p. 1145-1155, 2002.

[16] Howatson, A.M., Lund, P.G. and Todd, J.D., *Engineering Tables and Data,* London; New York: Chapman and Hall, 1991.

[17] Vander Voort, G.F., *Metallography Principle and Practice*. ASM International, 1999. p. 623.

[18] Shan, X., Watkins, J.J., "Kinetics of Cuprous Oxide etching with β-diketones in Supercritical CO_2", *Thin Solid Films,*Vol. 496, p. 412-416, 2006

3.11.2 Figure capture

Figure 1. The image shows the microstructure of 99.9% copper used in this study. The grain size is relatively large and the average grain size is approximately 25 microns.

Figure 2. The schematic of the experiment setup consist of four elements: Base, C-clamp, capacitance gage, rollers and sample. A load is generated thought the C-clamp when the rollers and samples are placed in between the frame and extrusion of the base.

Figure 3. The schematic shows compressive stress is generated at the top of the sample and tensile stress at the bottom of the sample.

Figure 4. Tip radius is characterized. The images show the tip radius change in x and y direction before (a and b) and after (b and c) the experiment.

Figure 5. Force curve taken before the initial AFM topographical image was taken showing the force distribution and adhesive force.

Figure 6. The images show: (a) Initial 5µm x 5µm scan. (b) Final 5µm x 5µm scan with scratched area shown. (c) Subtraction of initial image from final image and three-dimensional image showing height difference.

Figure 7. Three-dimensional image showing trench depth.

Figure 8. Graph showing the material removed by the wear plotted against surface stress state in ambient condition. The material removal is accelerated by compressive stress and suppressed by tensile stress. It also shows the material removal is linearly affected by the surface stress state.

Figure 9. Schematic of the hypothesized damage mechanism occurring as the AFM probe scratched across the sample surface in ambient condition.

Figure 1.

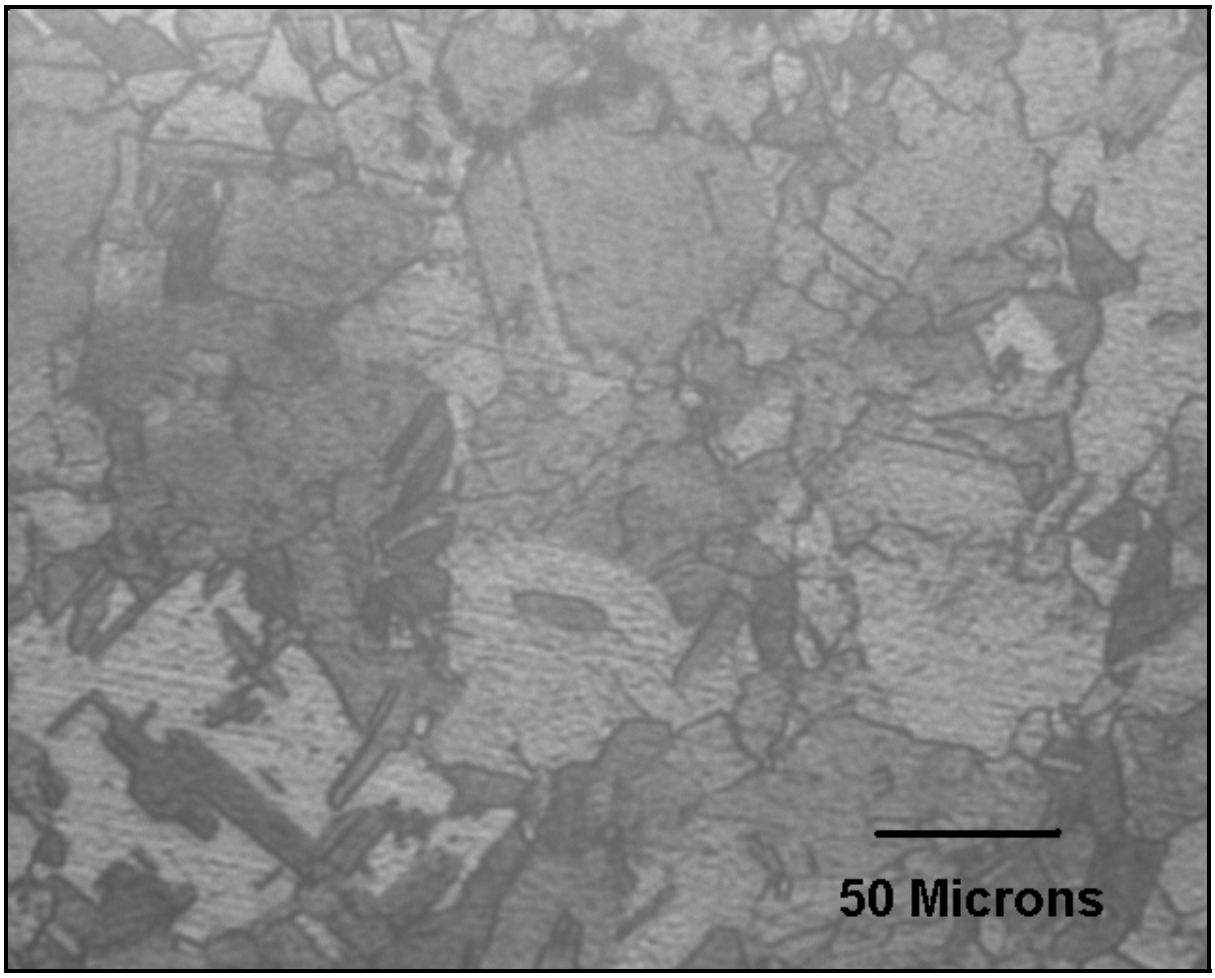

Figure 2.

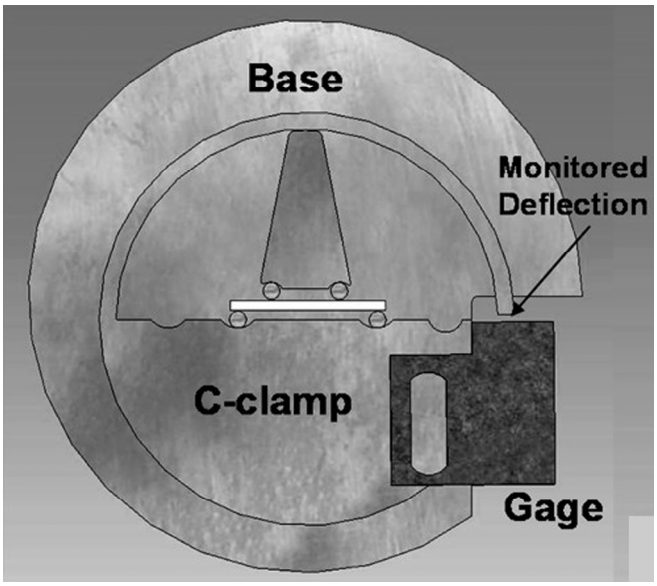

Figure 3.

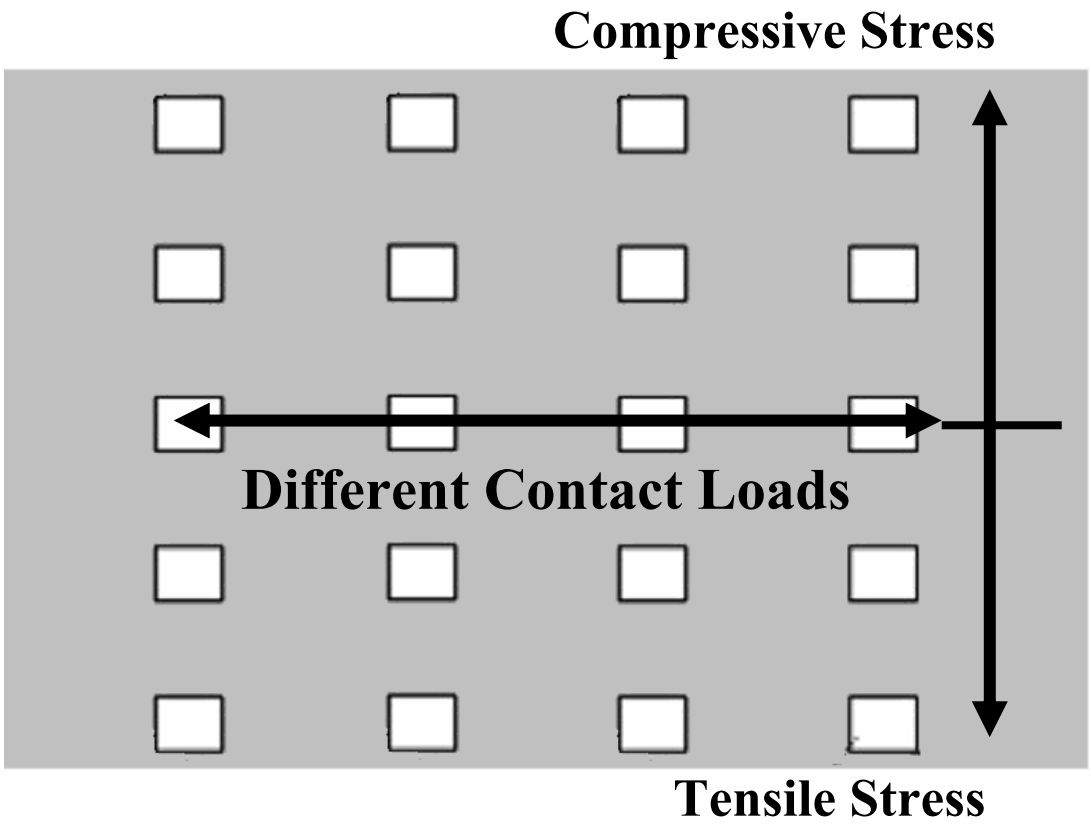
Compressive Stress
Different Contact Loads
Tensile Stress

Figure 4.

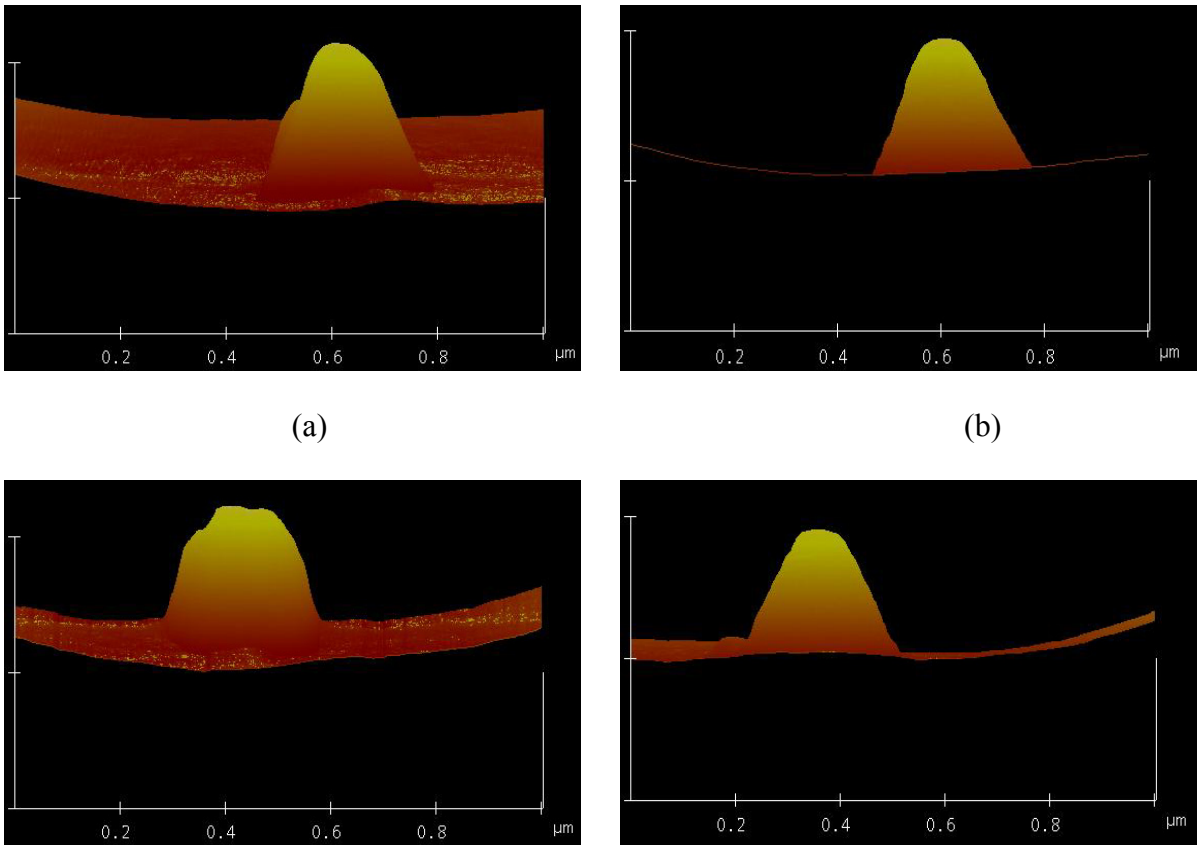

Figure 5.

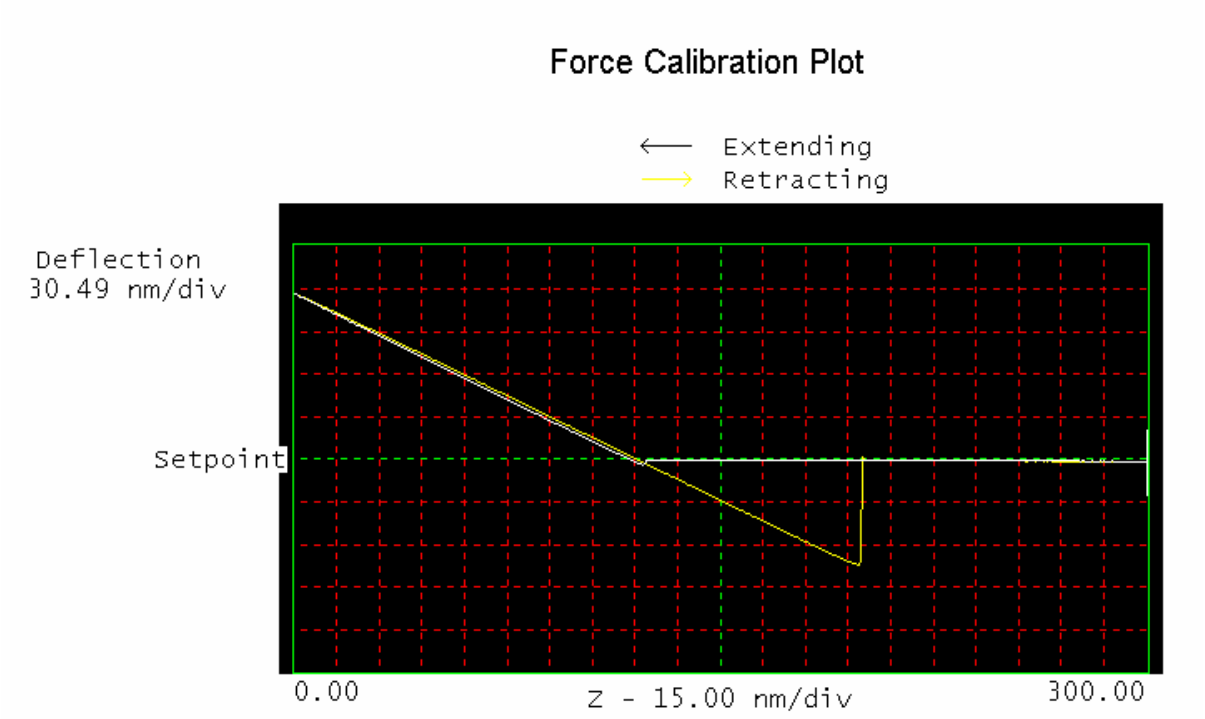
Force Calibration Plot
Extending
Retracting
Deflection
30.49 nm/div
Setpoint
0.00
Z - 15.00 nm/div
300.00

Figure 6.

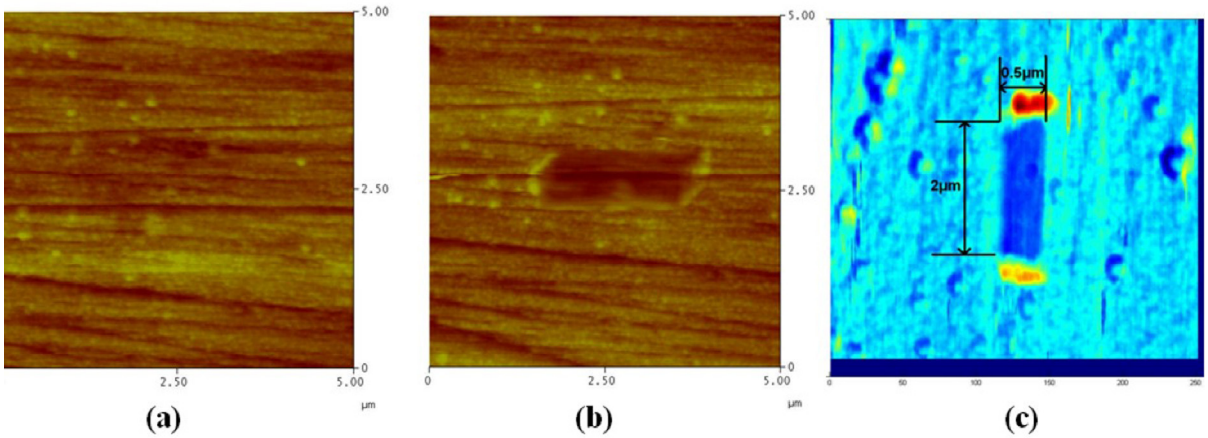

Figure 7.

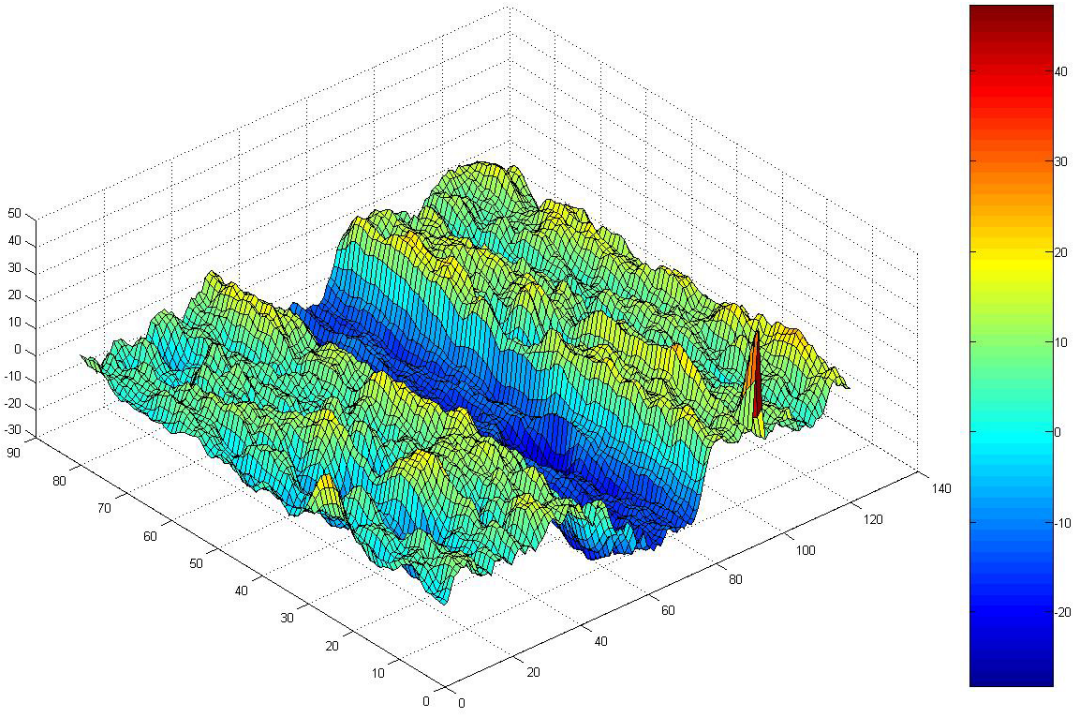
50
40
30
20
10
0
-10
-20
-30
90
80
70
60
50
40
30
20
10
0
0
20
40
60
80
100
120
140
40
30
20
10
0
-10
-20

Figure 8.

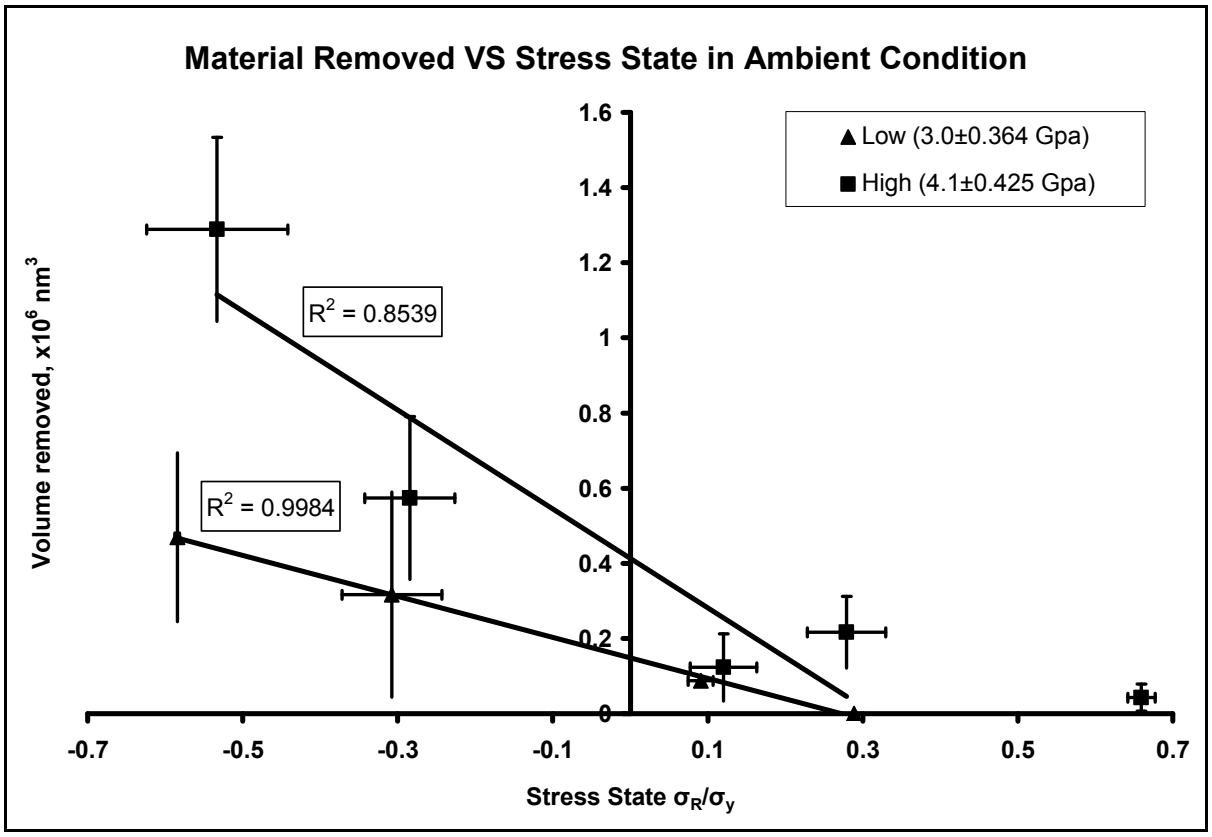
Material Removed VS Stress State in Ambient Condition
Low (3.0±0.364 Gpa)
High (4.1±0.425 Gpa)
R2 = 0.8539
R2 = 0.9984
Volume removed, x10^6 nm^3
Stress State σR/σy
1.6
1.4
1.2
1
0.8
0.6
0.4
0.2
0
-0.7
-0.5
-0.3
-0.1
0.1
0.3
0.5
0.7

Figure 9.

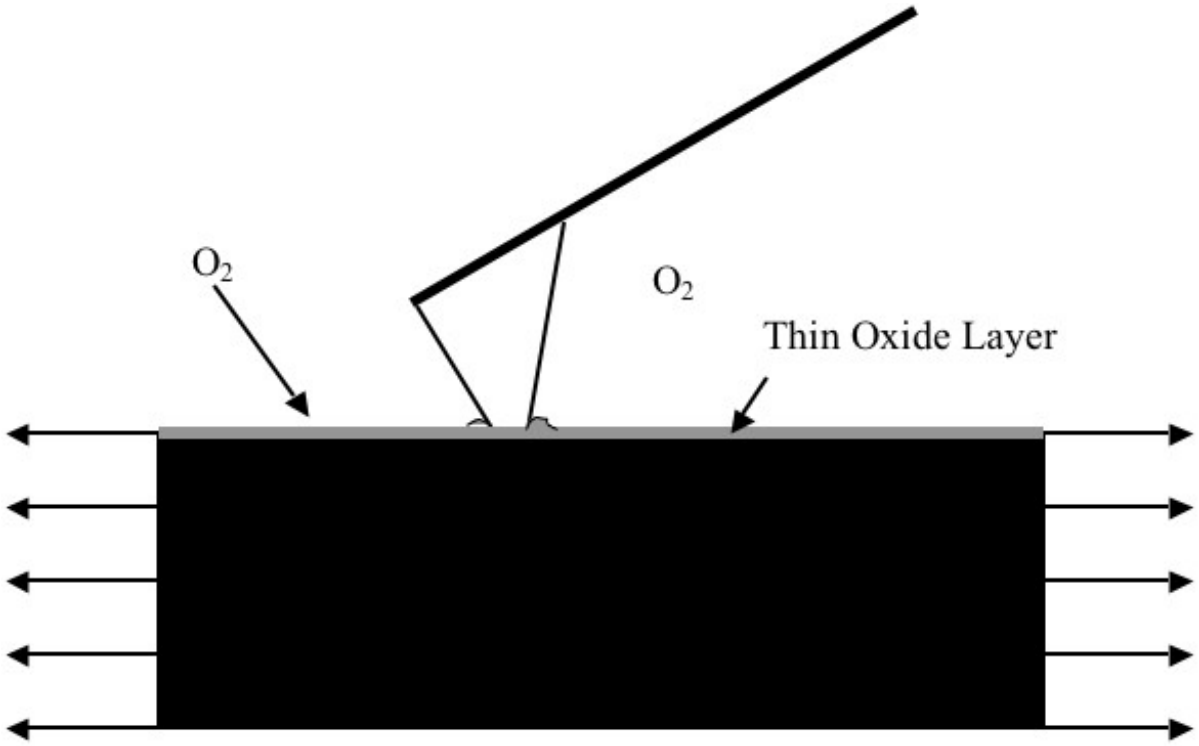

CHAPTER 4: LOAD ASSISTED DISSOLUTION AND DAMAGE OF COPPER SURFACE UNDER SINGLE ASPERITY: INFLUENCE OF CONTACT LOADS AND SURFACE ENVIRONMENT

A paper to be submitted to Journal of The Electrochemical Society

Bun-Hiong Chua, Pranav Shrotriya, Abhijit Chandra
Mechanical Engineering Department, Iowa State University 2007

4.1 Abstract

An experiment setup was used to investigate the effects of contact loads, surface stress state and surface environment on dissolution and damage of copper surface. A range of surface stress state was generated with a four-point-bending setup on a well-polished copper sample. Single asperity contact was investigated using the cantilever tip of an Atomic Force Microscope. Controlled tip contact pressures were applied on the copper surface to mechanically stimulate the stressed surface. Different contact pressures applied on the sample can be calculated by measuring the loads applied and the radius of the cantilever. The experiment was performed in different environments to determine the chemical effects. Volume of material removed during the process was measured to determine material removal rate as a function of contact pressure, surface stress state and environment conditions. It shows, as expected, higher contact pressures accelerate the material removal rates. With constant pressure in slightly acidic de-ionized water, the wear rates accelerate significantly at the compressed as well as stretched surface, which gives a deep parabolic graph. In basic environment, Ammonium Hydroxide, the wear rates are almost independent of surface stress state and only affected by the contact pressure. Mechanics governing material removal and their removal to Chemical Mechanical Polishing (CMP) of copper was discussed.

4.2 Introduction

Copper has become a widely used material in advanced submicron multilevel technologies due to its low resistivity and high electromigration resistance [14]. Therefore, researches have been done to investigate different processing methods in submicron integrated circuit manufacturing of copper. Copper based devices are manufactured using additive patterning and subsequently undergo chemical mechanical planarization (CMP) to ensure good interconnection [1]. CMP has grown rapidly as part of mainstream processing methods [11]. During CMP, material is removed through synergistic combination of chemical reactions and mechanical stimulations. Empirical models such as Preston's equation [2] are used to explain the material removal rate during CMP but a mechanism based understanding of the synergistic interactions between chemical environment and mechanical loading is still lacking.

During CMP, the process experiences two possible contact modes: hydrodynamic and solid-solid contact modes. For hydrodynamic contact mode, the polishing pad has no contact with the material surface leaving the abrasives in the slurry mechanically stimulate the surface. In this case, material removal rate is greatly influenced by the number of active particles during the process, which follow the flow of the slurry closely. In solid-solid contact mode, the polishing pad is in contact with the surface of the material together with the abrasives. The abrasives' contact pressure in this mode is usually higher compared to the hydrodynamic contact mode. Each active particle contributes to the overall polishing process and therefore, it is necessary to investigate the polishing process under single asperity in order to get a better understand of the mechanism.

Besides the effect of mechanical abrasion of the active particles, chemical reactions play an important role in determining material removal mechanism during mechanical stimulation. CMP needs to fulfill the following chemical conditions in order to achieve good surface planarization: (a) The metal must undergo a rapid repassivation in the slurry, (b) Active dissolution only take place at the upper surface site- the passivated layer is removed by the direct contact of the abrasives and (c) Repassivation of the activated sites in the slurry [15].

The surface condition is highly affected by the pH of the solution. Pourbaix diagram [3] is usually used to determine the pH needed for specific research purpose. In this experiment, it is important to investigate the mechanism of material removal in each of the chemical conditions. According to the copper Pourbaix diagram, copper surfaces are passivated with formation of a hydrated oxide layer in alkaline solution. When the surface is mechanically stimulated, it removes the oxide layer on the top of the surface. The surface is then being reactivated and forms another oxide layer. The process of abrasion and repassivation is repeated leading to material removal. However, in acidic solution, copper surfaces undergo rapid etching as the formation of oxide passivation layer is not preferred thermodynamically. The surface of copper is etched continuously and causes the surface to be unstable. Therefore corrosive inhibitor is needed to prevent the material to be dissolved completely. This inhibitor can mimic the behavior of a passive oxide layer during CMP. One of the commonly used inhibitors for copper in acidic slurries is benzotriazole (BTA). It is shown that BTA tends to react with copper and form Cu-BTA layer on the surface. The Cu-BTA layer will serve as oxide later in the abrasion-passivation mechanism [5-7]. When the inhibitor layer is removed from the surface of copper sample, it allows the chemical to react

with the material, which results active dissolution on the bare surface [16-18]. At the same time, the sample surface experiences rapid repassivation by the inhibitor. Hence, material removal in acidic slurries containing BTA proceeds through abrasion of passivating layer by mechanical abrasion and rapid etching and rapid repassivation of the exposed bare copper surfaces. Moreover, previous investigations have shown that, the chemical reaction rate is affected by the applied surface stress state of the sample [4,12]. However, the investigation of the chemical reaction rate due to the influence of surface stress state is still unclear.

The focus of this study is to investigate the influence of contact pressure and surface stress state on surface delamination and dissolution of polished copper in a single asperity contact mechanical stimulation. In the present study, a four-point-bending fixture is used to generate a range of surface stress states. Atomic Force Microscope (AFM) and silicon nitride cantilever are used to model the single asperity wear with several applied loads on a 99.9% copper sample. The effects of both contact pressure and surface stress state are investigated by conducting experiment with different contact loads applied with AFM in different chemical environments. The experiment preparation and setup are discussed in the following sections. The measured material removal as a function of contact loads, surface stress state and environment are presented and the implications of experiment results are discussed.

4.3 Experimental Setup and Equipment

4.3.1 Material and Sample/ Chemical Preparation

The material used in this study is 99.9% pure copper. The samples were cut out from a 2.5mm think copper plate into 1.25mm x 2.5mm x 25mm in the thickness, depth and length respectively rectangular bars. The mechanical properties of copper are shown in table (1) [13, 23]. The 1.25mm thickness of the beam was polished with 600 grit with water, then with 3μm diamond suspension and lapping oil on nylon pad and finally with 0.05μm alumina suspension and de-ionized water on Microcloth. The samples were polished to a mirror finish. AFM image show the initial polished surface has a root mean square roughness of 4-6nm. Due to the nature of copper, it is almost impossible to eliminate the scratches produced during the polishing process. Several copper samples were etched with 1g FeCl3, 10mL HCl and 100mL water [8] to determine the average grain size. The microstructure is presented in figure (1) and reveal large grain size, in this case approximately 25micron.

Solutions used in the present study are de-ionized water, ammonium hydroxide and nitric acid plus BTA. Solution pH was measured before and after each experiment to monitor possible pH changes during the process. The open circuit potential (OCP) was measured with saturated calomel reference electrode (SCE) for each chemical.

4.3.2 Four-Point Bending Fixture

A four-point-bending fixture was use in this experiment. It consists of: the base, C-clamp, a capacitance gage (Capacitec, Myer, MA) and four rollers (modified pin gages from Meyer's Gage Company, South Windsor, CT). The setup was used to generate a range of surface stress state from compressive to tensile stress across the sample. The schematic of the

fixture is presented in figure (2). When the rollers and sample were placed in-between the C-clamp and the extrusion of the base, it forced the C-clamp to open and the free-end deflection can be monitored. A load was generated from the C-clamp to the sample. The load was determined by first calibrating the C-clamp with dead weight method. Different weights were used to determine the C-clamp free-end deflection as a function of load. The relationship between load and free-end deflection is

$$P = 0.024\delta$$

where P is the applied force and δ is the deflection in Newtons and microns respectively. Several sizes of roller were used to achieve the desired surface stress state. The mechanical properties of 99.9% copper are shown in table (1). The maximum applied surface stress is limited to 70% of the material yield strength, which is about 49Mpa. By knowing the geometries of the sample, the applied surface stress ca be calculated based on the load generated from the C-clamp. The surface stress of a specific location can be calculated according to its distance away from the neutral axis. As shown in figure (2), compressive stress is generated at the top of the sample and tensile stress at the bottom of the sample. The edges of the sample indicate the maximum stresses applied.

4.3.3 Atomic Force Microscope (AFM)

Single asperity wear of 99.9% pure copper was modeled with an AFM tip. A Dimension 3100 atomic force microscope with Nanoscope IV controller (VEECO Instruments, Woodbury, NY) was utilized for this experiment. In order to protect the piezoelectric scanner of the AFM, a fluid cell and polymer protective skirt were used in all experiments run in aqueous condition. A specially designed tip holder was use to prevent the

solution from interacting with piezoelectric scanner. Silicon nitride (Si_3N_4) cantilevers with a reflective gold backside coating (DNP-S VEECO Instruments, Woodbury, NY) were used in the present study. The cantilever with nominal spring constant of 0.58 N/m and nominal tip radius of 30 nm were used in this study. Although the manufacturer stated the stiffness of the cantilevers to be 0.58nN/nm, but the cantilevers were experimentally calibrated to ensure the accuracy of the results. The deflections of the cantilever when applying on a hard sample (sapphire) and reference cantilever were recorded and compared. The actual cantilever stiffness can be calculated with the equation:

$$k_{cantilever} = \frac{(\delta_{Sapphire} - \delta_{RC})}{\delta_{RC}} * (k_{RC})$$

where 'δ' is cantilever deflection and subscript '*RC*' refers to the reference cantilever. The tip radius of each cantilever was characterized by scanning on a silicon tip characterizer TGT01 with radii curvature of less than 10nm. The probe wear during the experiment can be determined by monitoring the tip radii before and after each experiment. An example of the tip AFM image is presented in Figure (6).

4.4 Experiment procedures and Data Analysis

The sample and rollers were inserted in-between the C-clamp and the extrusion of the base. The free-end deflection of the C-clamp was monitored by the capacitance gage to determine the applied stress across the sample surface. Since the objective of this study if to investigate the effects of contact load, surface stress state and environments on material removal, the experiments were performed with four different loads applied by the AFM (15nN, 30nN and 60nN) and at five different surface stress states. The sample was placed

under an optical camera to identify the specific scan location based on the surface features and defects. The stress state of the scan locations were according to the distances away from the neutral axis. The surface removal rates were investigated in three different aqueous conditions. By referring to Pourbaix diagram in Figure (3), the solutions were chosen for different chemical reactions with copper: (a) Slightly acidic condition with De-Ionized water (pH 6), (b) Passivation condition with Ammonia Hydroxide (pH 9) and (c) Corrosion condition with Nitric Acid with inhibitor BTA (pH3). All the experiments were performed at room temperature approximately 23°C and 40% relative humidity. Chemical pH was measure before and after the experiment. The samples were covered with a masking tape with a window cut to fit the thickness of the sample to hold the solution in place. Only a few droplets of solution were needed just enough to cover the whole area of the sample surface for each test.

For each experiment, the cantilever stiffness was calculated and tip radius was analyzed before scanning on the copper sample surface. Due to the AFM drifting problem, the AFM was warmed up for about one hour or until no noticeable change in scanned location was observed during on multiple scans on the same area. This was only necessary before a set of data was obtained. To be consistent of all tests, the scan angle is set to 0°. Force curves for all the experiments were recoded right after the cantilever tip was engaged with the sample surface to monitor any possible external forces such as pull-off force. An initial 5μm X 5μm topographic scan was obtained. The AFM image was used to determine the surface feature and roughness. With contact load as low as 1-2nN, no material was removed from the surface. Slow scan speed, 2Hz, was used for the initial image. The initial image was recorded. A scratching process was then performed in an area of 2μm X 0.5μm at

the center of the 5µm X 5µm scanned area with the desired contact load and a speed of 5Hz for 15 minutes. After the scratching process, the setup was reset back to the parameter used to take the initial image. A 5µm X 5µm final topographic image was recorded. The scratch/ delamination was done starting with the lowest contact loads, 15nN. The process was repeated with different surface stress states, strong compressive, weak compressive, neutral, weak tensile and strong tensile stress states. The tip radius after all the five experiments was measured. With constant contact load, the scans were performed across the sample from compressive stress state through tensile stress state. This is to ensure the cantilever was undergoing a consistent load and can be assumed that the probe wear rate was distributed evenly for each scratch. The average probe wear can be calculated by dividing the total probe wear by the number of tests performed, in this case, five tests on five different stress states. Then, the experiments were repeated with higher contact loads. Since the probe wears for 15nN were minimal, the cantilever was reused for 30nN. A single cantilever was needed for 45nN and 60nN due to the high probe wear rates. The loads were then converted to contact pressure according to the tip radius during the scratch. With a constant contact load, the applied contact pressure was higher for the shaper tip probe compared to the blunted tip. After gathering all the contact pressure values, they are grouped into 3 pressure ranges: Low, Medium and High contact pressures. Unlike the experiments performed in ambient condition, no adhesive force was observed in the force curve leading a conclusion that no external forces were applied to the sample other than the loads directly applied by the AFM. The value will serve as the actual force for the contact pressure analysis. An example of force curves obtained in aqueous condition is shown in Figure (4).

Since the AFM drifting problem is unavoidable, the final image was registered to match the initial image. Although the sample was polished to be a smooth surface, but because of the softness of copper sample, scratches and adhesive tear produced by the polishing process could not be totally eliminated. Therefore, they were used to be the reference points for the image registration. The initial image was then subtracted from the final image to eliminate the effect of the surface features and impurities for the material removal rate analysis. After the subtraction, only the scratched area was clearly shown on the image. The initial image, final image and subtracted image are shown in figure (5). The material removed during the wear process can be determined by measuring the depth difference between the scratched and unscratched area. The average height of the scratched area was based on four measurements within the 2μm X 0.5μm window. The height of the unscratched area was measured at four different locations. The volume removed during the wear can be estimated from the subtracted image. A three-dimensional image of the subtracted image is presented in Figure (6).

4.5 Error Estimation

The trench depths are analyzed as a function of surface stress state for different contact pressure. The error bars shown in the figures were analyzed based on several effects. While the contact pressures were grouped into ranges, the average contact pressure was calculated based on the number of contact pressure in a particular pressure range. The error is plus and minus one standard deviation of the contact pressure values. As mentioned in the previous section, the geometry of the AFM tips was characterized before and after each experiment. The probe wears are very consistent to follow the manner where less wear

occurs with the lower contact pressures. The largest probe wear was noted in the highest contact pressure, in this case, 60nN.

Also, the uncertainty in the surface stress values was conservatively estimated by taking into account the deviations of the load applied by the C-clamp, sample geometry and the camera used to determine the surface features discussed earlier. The error analysis associates with material removal rate are based on plus and minus one standard deviation of four different trench depth measurements. The results are discussed in the next paragraph.

4.6 Experiment Results

The volume of the material removed during the wear is plotted as a function of surface stress state. The result for each environment is presented in figure (8), (9) and (10) where they are obtained in aqueous condition of pH 6, pH 9 and pH 3 respectively. The chemical environments are determined based on the Pourbaix diagram [3], which indicates corrosion condition in acidic solution and passivation in alkaline solution. The OCP were measured with saturated calomel electrode and they are presented in Table 2. The isoelectric point of copper oxide is about pH 9.5 [24]. DI water drops on the boundary between passivation and corrosion on the Pourbaix diagram and ammonium hydroxide indicates passivation region. The OCP of the nitric acid decreases from $0.252V_{SHE}$ to $0.144\ V_{SHE}$, which indicates the surface reaction changes from corrosion to nearly immunity. The chemical selection gives a very good variety of material reactions in order to study the environment effect in this study.

To better understand the wear rate of the experiment, it is necessary to compare the different contact pressures rather than contact loads. This is due to the tip shape and radius of

each cantilever used was different. Hertzian contact analysis was used to estimate the average contact stress based on the contact load and radius. The material properties of copper and tip material (Si_3N_4) are shown in table (1). Since the tip radius of each tip changes dramatically during the wear process, it was impossible to maintain the contact pressure ranges for all the chemical environments.

For pH 6 DI water experiment, the applied contact pressures are grouped into three categories: low (2.783±0.096Gpa), Medium (3.446±0.292Gpa) and High (4.088±0.242Gpa). As shown in figure (7), the wear only started to appear at contact pressures of more than 3Gpa. As the contact pressure increases, the material removal increases. With higher contact pressures, medium and high, it is very interesting that both compressive and tensile surface stresses accelerate the material removal but compressive stresses have more pronounced effect compared to tensile stresses.

Figure (8) shows the obtained in alkaline environment, pH 9 ammonium hydroxide. The contact pressures were grouped into three pressure ranges, Low (2.755±0.022Gpa), Medium (3.458±0.103Gpa) and High (4.305±0.182Gpa). At the lowest contact pressure, no noticeable damage on the surface is observed. As expected, increase in contact pressure accelerates the material removal rate. For contact pressure greater than 3Gpa, the wear rate is almost independent (slightly quadratic dependent) of surface stress state and only affected by the contact pressure. The result indicates that under passivation condition, surface chemical reactions are not influenced by the surface stress state and mechanical abrasion determines the material removal rate.

The trench depth of the scanned area was plotted against surface stress state for experiment performed in acidic solution (nitric acid with pH 3). The result is presented in

figure (9). Due to copper is very reactive with nitric acid, corrosion inhibitor (BTA) was added into the solution. The material removal increases with increase in contact pressure. Unlike the previous results, the material on the surface was being removed during the scratching process with the lowest contact pressure (2.835±0.049Gpa). The result shows very interested wear rate distribution in acidic environment (pH3) where both compressive and tensile stresses suppress the material removal.

4.7 Discussion

The primary objective of this study is to investigate the effects of surface stress state and environment during single asperity wear of copper sample. In order to achieve the goal, the experiments were performed in various chemical environments with fixed contact loads and surface stress states. The material removal was analyzed based on three chemical environments: slightly corrosive condition in slightly acidic de-ionized water (pH 6), passivation condition in basic ammonium hydroxide (pH 9) and corrosive condition with inhibitor in acidic nitric acid plus BTA (pH3).

The pH of the solution before and after the test was recorded and the measurement shows the Ph of de-ionized water is around 6, which is different from the pH of pure water (pH 7). When de-ionized water is exposed to the atmosphere, it reacts with carbon dioxide in the air and form carbonic acid. As a result, it follows the manner of corrosion condition. When the sample is placed under slightly corrosive condition, no damage was observed for the lowest contact pressure (2.783±0.096Gpa). The finding is different compared to the previous work done where the minimum required contact pressure to dislocate copper is about 1.6Gpa [20]. This is significantly affected by the formation of oxide layer and its

mechanical properties. It is observed that the wear rate was accelerated by both compressive and tensile surface stress states. The results show that the material removal rate on the compressive stress side is slightly higher than the tensile stress states. During the scratching process, surface damage proceeds through superposition of two different surface process (mechanical stimulation and chemical reaction: In ambient non-reactive condition, the results obtained shows linear distribution across the sample surface where the compressive stress accelerated material removal and tensile stress suppress the process [19] and chemical reaction has quadratic dependence on surface stress state leading to the skewed quadratic dependence of surface stress state as observed.

In passivation condition, the results also follow the manner where no surface damage is observed for the lowest contact pressure range (2.755±0.022Gpa). Approximately 3Gpa contact pressure was needed to remove material both in slightly acidic and alkaline solution. However, the material removal in alkaline shows very slight influence by the surface stress state and mainly affected by the contact pressure. The results indicate that the chemical reaction is slightly influenced by the surface stress state and mechanical abrasion determines the material removal. Therefore, during CMP, the chemical reaction is uniform in all regions. Surface planarization is still achievable because the peaks of the surface experience higher contact pressure than the troughs resulting higher material removal at the peaks. Therefore, the height difference between the peaks and the trough becomes less as time goes by.

The result obtained in acidic solution is very interesting as compared to the previous two chemical environments. Copper is very reactive with nitric acid where the oxide layer is corroded continuously and the sample surface become unstable. Therefore, BTA was added as a corrosion inhibitor. When copper sample is exposed to nitric acid + BTA, BTA tends to

react with copper and Cu-BTA layer is formed on the surface of the sample. This film serves as the oxide layer and fulfills the required condition of rapid repassivation on the sample surface [15]. The phenomena observed in this study is consistent as compared to the previous works where the BTA forms a protection layer between copper and solution and prevent chemical reaction [5,6]. As shown in Figure (9), the material removal was suppressed by both compressive and tensile stress. The result indicates that the reaction of BTA and copper is more rapid on the stressed surface than the unstressed surface. Figure (5) (C) shows the subtracted image of the test performed in acidic condition. Since the scan angle is 0°, the pile-ups appear on the side are believed to be Cu-BTA where the film was mechanically drag to the edges of the 2μm X 0.5μm window. The pile-ups observed in the ambient, slightly acidic and alkaline solutions appeared to be much less then in acidic solution. It is believed that when the surface is mechanically abraded, the surface is also chemically corroded leading to more material being removed during the process. At the sample time, BTA react with the copper before it escapes from the surface. The observed pile-ups in acidic solution are more apparent. As known the average thickness of the Cu-BTA layer in acidic solution is thicker than 1000nm when the material is exposed to the solution for a long time [14]. Therefore, according to the results, only the Cu-BTA layer was being removed during the wear test.

Results show CMP is unstable in the corrosive condition without inhibitor. As shown in previous work [4], the material surface becomes unstable when the surface is stretched and exposed to corrosive solution. When a stress is applied, the maximum stress appeared to be at the troughs rather than at the peaks. The etch rate in the troughs of the stretched surface is accelerated while the etch rate is suppressed at the peaks by the tensile stress leading increase

in height difference between the peaks and troughs. While in compressive stress, the result shows different manner where compressive stress also accelerates the etch rate in this investigation. The passivation condition has minimal influence in chemical reaction rate and only affected by contact pressure. Experiment performed in acidic with inhibitor added solution shows the interesting relationship between surface stress state and chemical reaction rate. The sample encounters both corrosion and passivation at the same time. It is believed that both compressive and tensile stresses suppress the etching reaction and accelerate passivation process. Since the maximum stress (compressive or tensile) is at the troughs of the surface, based on the observation in this experiment, less material is removed at the trough and more material is removed at the peaks of the surface resulting decrease in height difference between peaks and troughs and produces planarization. Since more contact pressure is applied at the peaks, the material removal rate appeared to be higher. By utilizing both chemical and mechanical effects, CMP with acidic plus inhibitor is the ideal solution. The abrasion process with the AFM cantilever tip in different environments is schematically explained in Figure (11).Table 3 shows the results comparison in the current study and previous work [7]. Since the results were obtained in different contact pressure and environment condition, the results may not be compared directly. However, it gives an idea of how copper reacts with different environments. As shown in Table 3, the results obtained with medium contact pressures were compared. Both of the results show the material removal rate is accelerated in corrosion (acidic) solution and suppressed by passivation (alkaline) solutions. Interestingly, there are mixed observations in the DI water. The measured pH in both cases are different. The pH of the DI water used in the present experiment is measured to be pH 6 where pH 7 in the other case. Therefore, the material is

undergoing different chemical reactions and mechanical stimulation. According to Preston's equation, the results were normalized based on the relative velocity. The results obtained in the current study only reflect a single asperity wear. Therefore, in order to compare the two results, the number of active abrasives is needed. The ratio between the two results is shown in Table (4). The ratios are contributed by the number of active abrasives and the different contact pressures of each particle. Due to different surface reaction and pH of the surface, the results obtained in water are not comparable. However, the material removal results in ammonium hydroxide and nitric acid + BTA are compared. The differences between the ratios are minimal, leading to the conclusion that, the results obtained in the present investigation is reasonable. Both results show the same behavior during the polishing process in different environments.

4.8 Conclusion

A unique setup was used to model a single asperity stimulation of copper influenced by contact pressure, surface stress state and chemical environment. 99.9% copper samples were used in this study. The samples were polished to a mirror-like surface to minimize the effect of surface roughness. The measurements were performed in four different contact load which to be converted to contact pressures. Higher contact pressures indicate higher material removal for all cases. With the same contact pressure, the experiment was repeated in five environments: Slightly acidic, basic and acidic environments. For pressure below 3Gpa, no surface damage was observed in the slightly acidic and basic environment. However, the dependence of surface stress state in material removal is very complicated changes with the chemical environment. In slightly acidic aqueous environment, the surface material removal

was accelerated by both compressive and tensile stress states leading to a skewed quadratic dependence on surface stress state. In passivation condition, the surface damage is almost independent of surface stress state and only influenced by contact pressure. In corrosive with inhibitor environment, the result shows very interesting distribution where both compressive and tensile stress states suppress the material removal. The effect of surface stress states is more significant in the corrosive with inhibitor environment where both rapid corrosion and repassivation happen at the same time. Both compressive and tensile stress states enhance the repassivation process and protect the surface from corroded.

4.9 Acknowledgment

The authors would like to thank Dr. Sriram Sundararajan and K.S.Kanaga Karuppiah for valuable discussion on the atomic force microscope experiments. This research is financially supported by Binger Research Fund and NSF Projects.

4.10 Reference

[1] Dejule, R., "CMP challenges below a quarter micron." *Semicond. Int.*. p. 54-60, 1997.

[2] Preston, F.W., *The theory and design of plate glass polishing machine*, J. Soc. Glass Technol., 1927, 11, No44, p. 214-256.

[3] Pourbaix, M., *Atlas of Electrochemical Equilibria in Aqueous Solution*, Pergamon Press, Cebelcor Brussels, 1966. p. 384-392.

[4] Yu, H.H., Suo, Z., "Stress-dependent Surface Reactions and Implications for a Stress Measurement Technique," *Journal of Applied Physics*, Vol. 87, Issue 3, p. 1211-1218, 2000.

[5] Carpio, R., Farkas, J. and Jairath, R., "Initial Study on Copper CMP Slurry Chemistries." *Thin Firm*, 266, p. 238-244, 1995.

[6] Luo, Q., Campbell, D.R. and Babu, S.V., "Chemical –Mechanical Polishing of Copper in Alkaline Media*," Thin Solid Films*, 311, p. 177-182, 1997.

[7] Steigerwald, S.P. Murarka, R.J., Gutmann, D.J. Duquette, "Chemical Processes in the Chemical Mechanical Polishing of Copper*." Material Chemistry and Physics*, 41, p. 217-228, 1995.

[8] Vander Voort, G.F., *Metallography Principle and Practice*. ASM International, 1999. p. 623.

[9] Tortones, M. and M. Kirk, "Characterization of Application Specific Probes for SPMs." *SPIE*. 3009: p. 53-60, 1997.

[10] Marinez, M.A., "Chemical-Mechanical Polishing: Route to Global Planarization*." Solid State Technology*, 37/5: p. 26-31, 1994.

[11] Che, W, Bastawros, A. and Chandra, A., "Surface Evolution during the Chemical Mechanical Planarization of Copper." *CIRP Annals- Manufacturing*, Vol 55/1, P. 605-608, 2006.

[12] Kim, K. S., Hurtado, J. A. and Tan, H., "Evolution of a surface-roughness spectrum caused by stress in nanometer-scale chemical etching." *Physical Review Letter*, 83: P. 3872-3875, 1999.

[13] Howatson, A.M., Lund, P.G. and Todd, J.D., *Engineering Tables and Data,* London; New York : Chapman and Hall, 1991.

[14] Ein-Eli, Y., Abelev, E., Rabkin, E. and Starosvetsky, D., "The Compatibility of Copper CMP Slurries with CMP Requirements." *Journal of The Electrochemical Society*, 150 (9) C646-C652, 2003.

[15] Kaufman, F. B., Thompson, D. B., Broadie, R. E. and Jaso, M. A. "Chemical-Mechanical Polishing for Fabricating Patterned W Metal Features as Chip Interconnects." *Journal of Electrochemical Society*, Vol. 138, 3460, 1991.

[16] Carpio, R., Farkas, J. and Jairath R., "Initial study on copper CMP slurry chemistries." *Thin Solid Film*, Vol. 311, p. 638,1995.

[17] Luo, Q, Mackay, R. A. and Babu, S. W., "Copper Dissolution in Aqueous Ammonia-Containing Media during Chemical Mechanical Polishing*." Chemistry of Material*, Vol. 9, p. 2101, 1997.

[18] Luo, Q., Campbell, D.R. and Babu, S.V., "Stabilization of Alumina Slurry for Chemical-Mechanical Polishing of Copper." *Langmuir*, Vol. 12, p. 3563-3566, 1996.

[19] Chua, B., Shrotriya, P. and Chandra, A., "Single Asperity Wear of Copper: Influence of Surface Stress State". Iowa State University, 2007.

[20] Bahr, D.F., Vasquez, G., “Effect of solid solution impurities on dislocation nucleation during nanoindentation*,” MRS*, Vol. 20, No. 8, p. 1947-1951, 2005.

[21] Aziz, M. J., Sabin, P.C. and Lu, G.Q., “The Activation Strain Tensor - Nonhydrostatic Stress Effects on Crystal-Growth Kinetics,” *Physical Review B*, vol. 44, pp. 9812-9816, 1991.

[22] Evans, U. R., *The Corrosion and Oxidation of Metals*, 2 ed. London: Edward Arnold Ltd., 1976.

[23] Ho, S. P., Carpick, R. W., Boland, T. and LaBerge, M. "Nanotribology of CoCr-UHMWPE TJR prosthesis using atomic force microscopy," *Wear*, vol. 253, p. 1145-1155, 2002.

[24] Lewis, J.A.,“Colloidal Processing of Ceramics”, *Journal of the American Ceramic Society,* vol. 83, no. 10, p.2341-2359, 2000

4.11 Table and Figure Capture

4.11.1 Table

Table 1

	99.9% Copper	**Si_3N_4 AFM probe**
Young Modulus	130Gpa	310Gpa
Poisson's Ratio	0.33	0.33
Yield Strength	70Mpa	-

Table 2

Chemicals	**OCP (V_{SHE})**	**pH**
DI water	0.173	6
Ammonium Hydroxide	0.137	9
Nitric Acid	0.252	3
Nitric Acid + BTA	0.144	3

Table 3

Environment	**Current Study** (Unstressed, medium contact pressure)	**Steigerwald et al** (multi asperity)
DI water	13.3 x 10^3 nm^3/min	0.4 mm^3/min
Ammonium Hydroxide	86.7 x 10^3 nm^3/min	0.2 mm^3/min
Nitric acid	-	0.6 mm^3/min
Nitric acid + BTA	156.7 x 10^3 nm^3/min	0.336 mm^3/min

Table 4

Environment	**Current Study** **600 µm/min** **(single asperity)(A)**	**Steigerwald et al** **78m/min** **(multi asperity)(B)**	**Ratio** **B/A**
DI water	2.22×10^{-8} µm^2	5.13 µm^2	231×10^6
Ammonium Hydroxide	1.44×10^{-7} µm^2	2.56 µm^2	17.8×10^6
Nitric acid	-	7.69 µm^2	-
Nitric acid + BTA	2.61×10^{-7} µm^2	4.31 µm^2	16.5×10^6

4.11.2 Figure capture

Figure 1. Microstructure of 99.9% copper used in this study. The grain size is relatively large with several grains reaching hundreds of micron and the average grain size is approximately 25 microns.

Figure 2. The schematic of the experiment setup consist of four elements: Base, C-clamp, capacitance gage, rollers and sample. The upper right inset shows the possible testing area and surface stress states were identified.

Figure 3. Pourbaix diagram of copper showing different chemical reaction process with different pH.

Figure 4. An example of force curve obtained before the initial image was recorded. No adhesive force was observed in all the force curves recorded during scanning process in aqueous conditions.

Figure 5. AFM image of: (a) Initial 5µm x 5µm scan. (b) Final 5µm x 5µm scan with scratched area shown. (c) Subtraction of initial image from final image.

Figure 6. Magnified three-dimensional AFM image showing clear scratched area.

Figure 7. AFM images showing tip radius changes (a) before and (b) after each experiment to monitor probe wear.

Figure 8. Graph showing material removal plotted as a function of various surface stress states with three contact pressure ranges in slightly acidic solution (pH 6). Error bars are based on one standard deviation of multiple measurements.

Figure 9. Results obtained in alkaline solution (pH 9). Material removal is plotted against surface stress states with three contact pressure ranges. Error bars are based on one standard deviation of multiple measurements.

Figure 10. Results of material removal plotted versus surface stress state in acidic solution (pH3). Estimated errors were based on one standard deviation of multiple measurements.

Figure 11. Schematic of the hypothesized damage mechanism occurring as the AFM probe scratched across the sample surface in: (a) slightly corrosive acidic environment, (b) passivation basic environment and (c) corrosion/passivation acidic environment.

Figure 1.

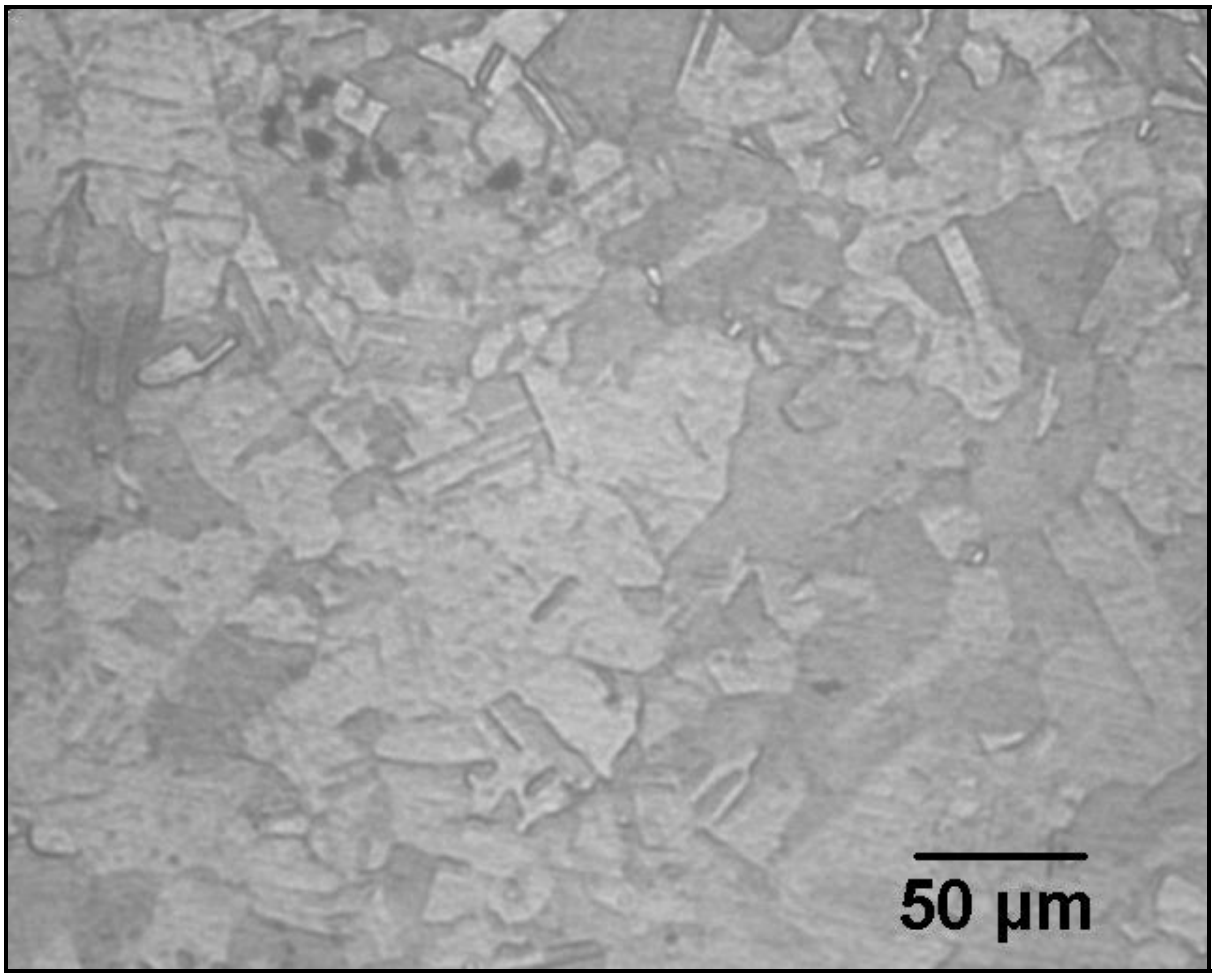

Figure 2.

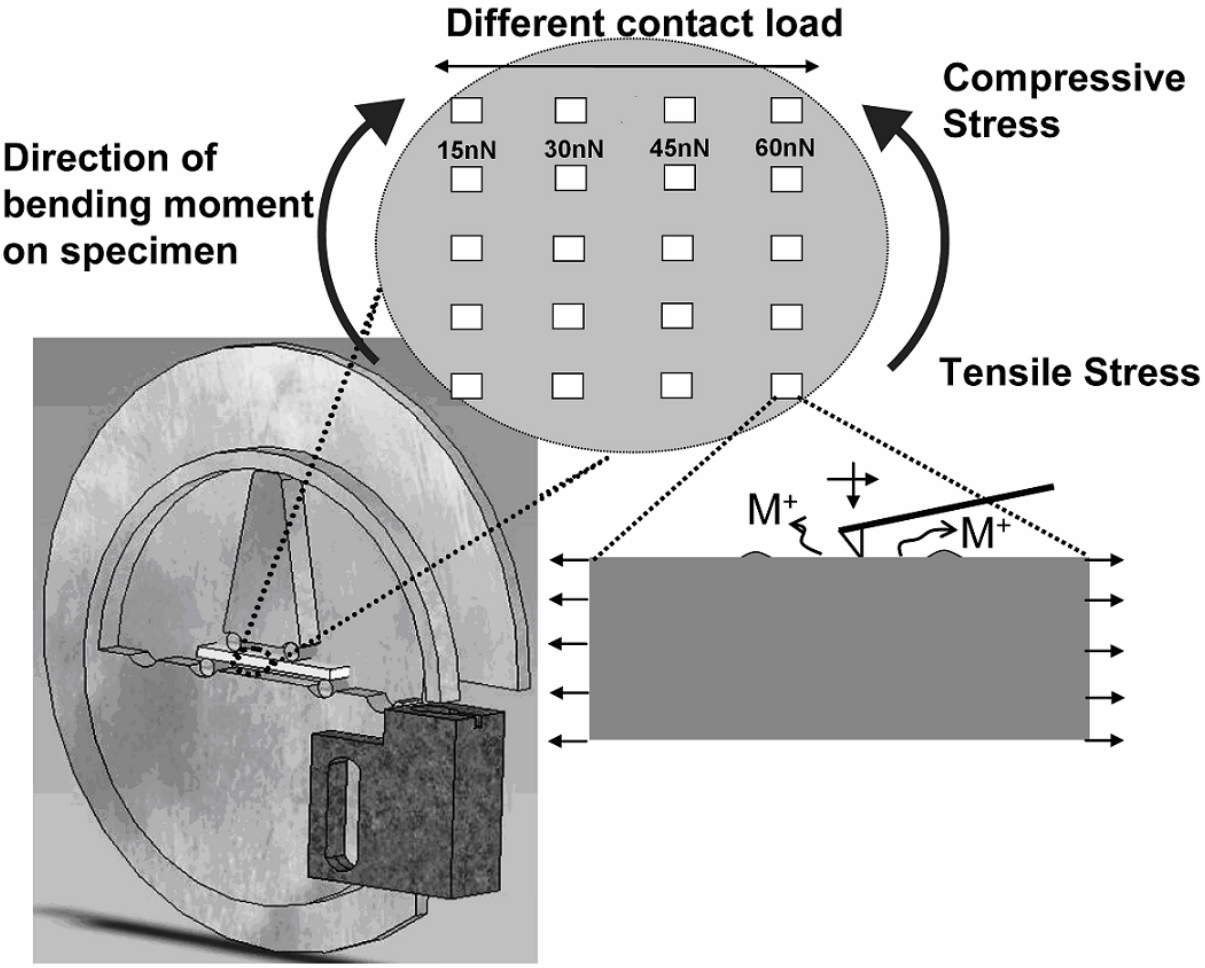
Different contact load
Compressive Stress
Direction of bending moment on specimen
15nN
30nN
45nN
60nN
Tensile Stress
M+
M+

Figure 3.

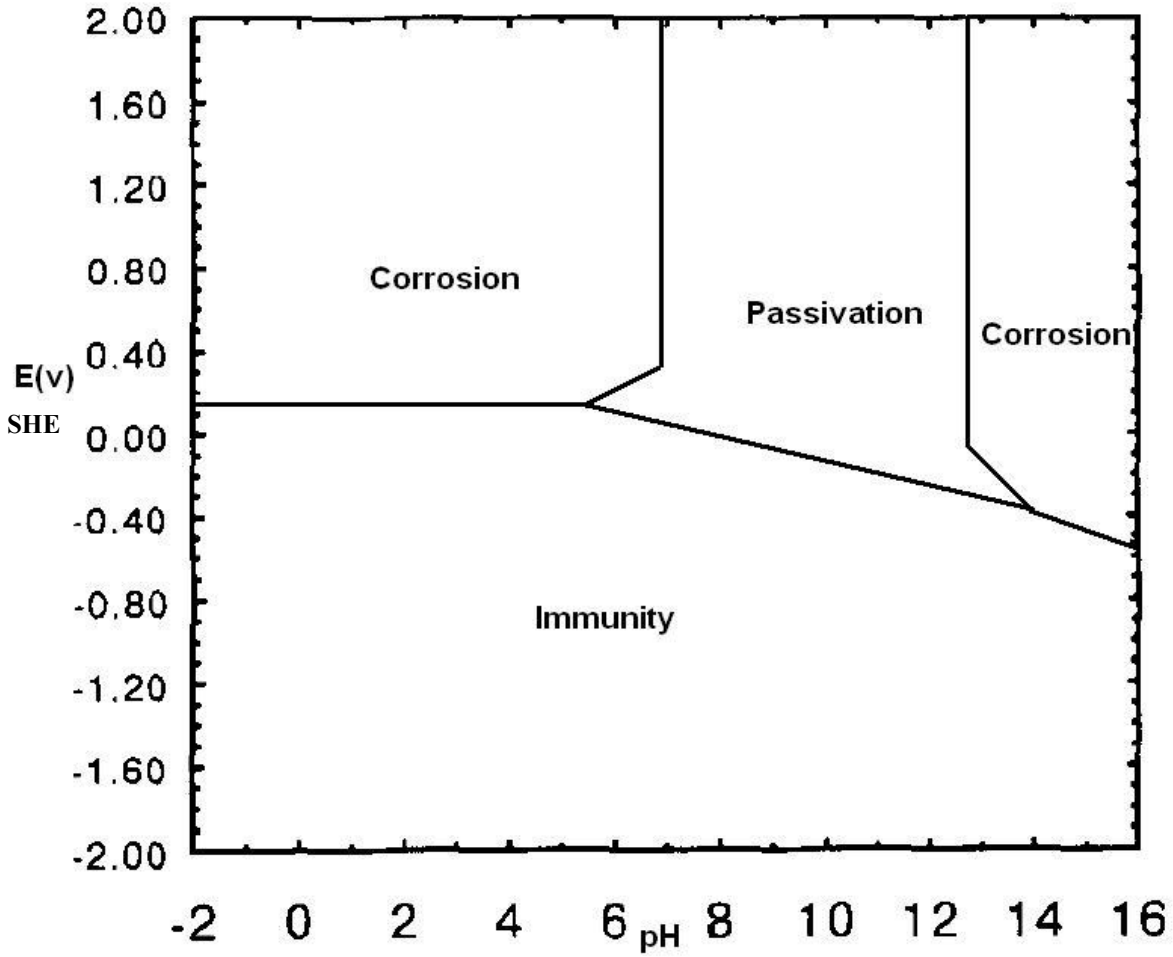
2.00
1.60
1.20
0.80
0.40
0.00
-0.40
-0.80
-1.20
-1.60
-2.00
E(v)
SHE
Corrosion
Passivation
Corrosion
Immunity
-2
0
2
4
6
pH
8
10
12
14
16

Figure 4.

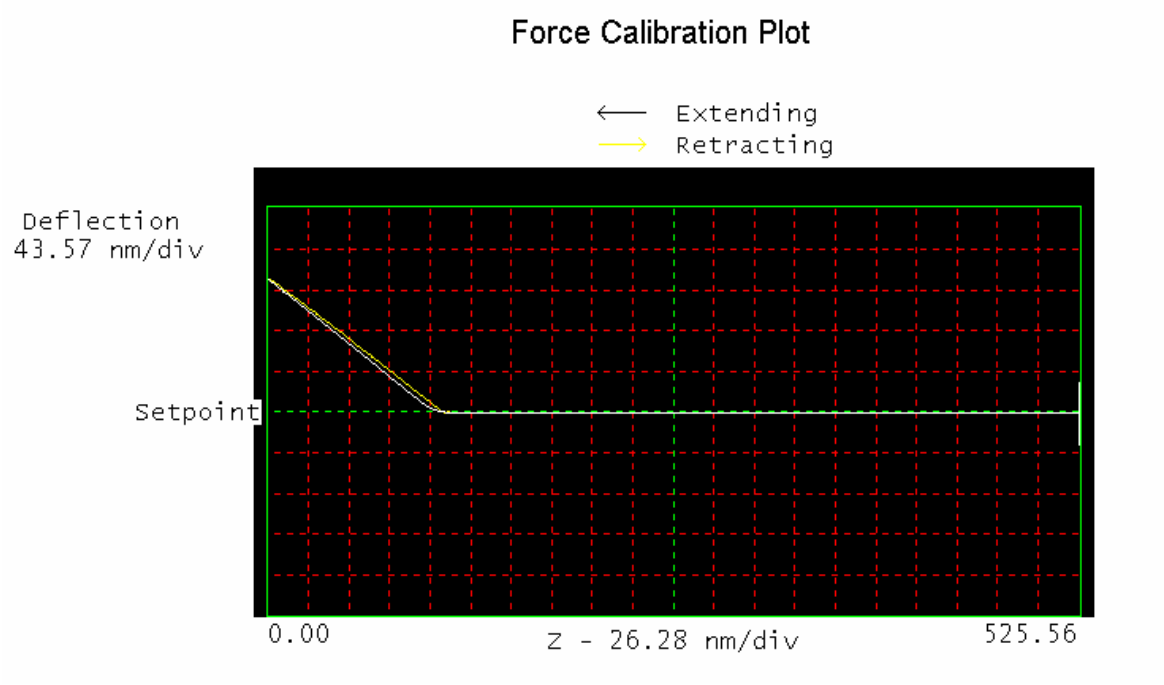
Force Calibration Plot
Extending
Retracting
Deflection
43.57 nm/div
Setpoint
0.00
Z - 26.28 nm/div
525.56

Figure 5.

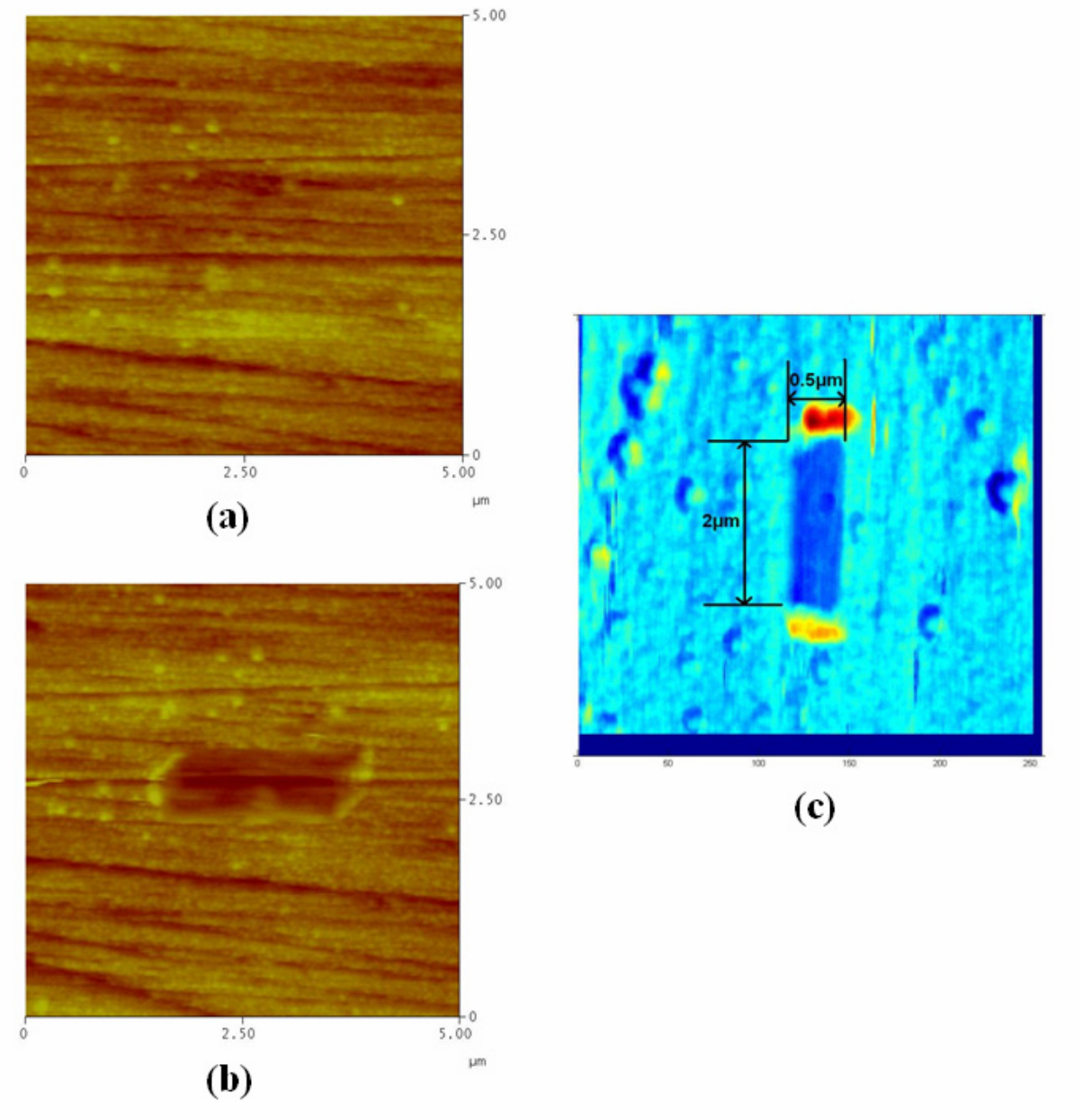

Figure 6.

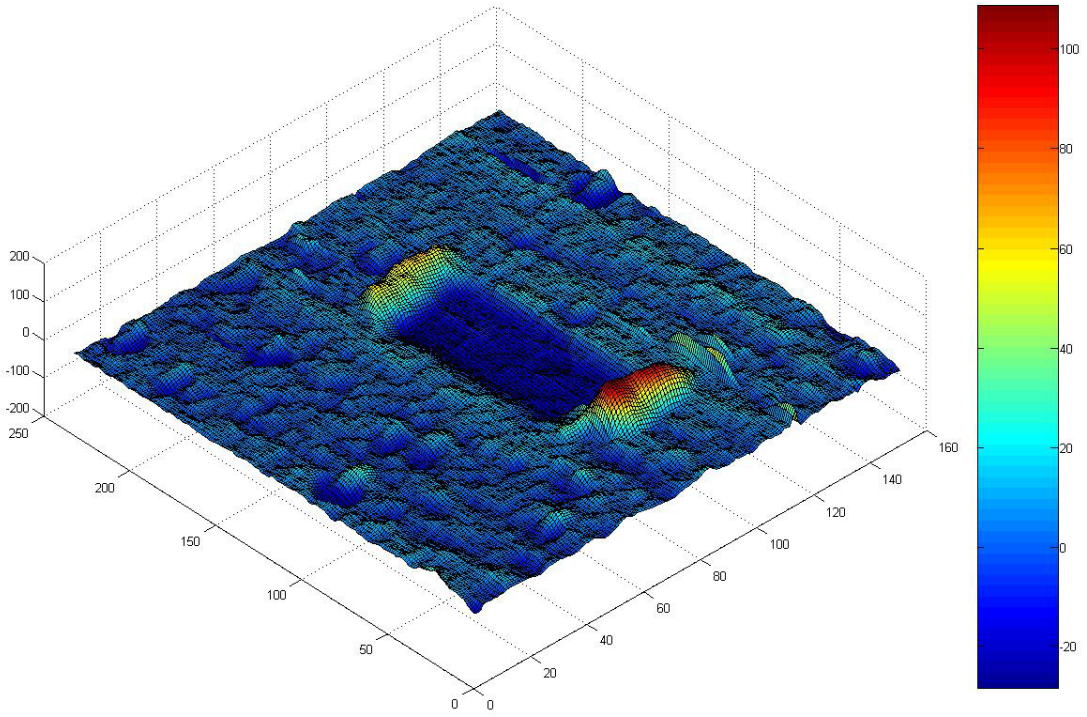
200
100
0
-100
-200
250
200
150
100
50
0
0
20
40
60
80
100
120
140
160
100
80
60
40
20
0
-20

Figure 7.

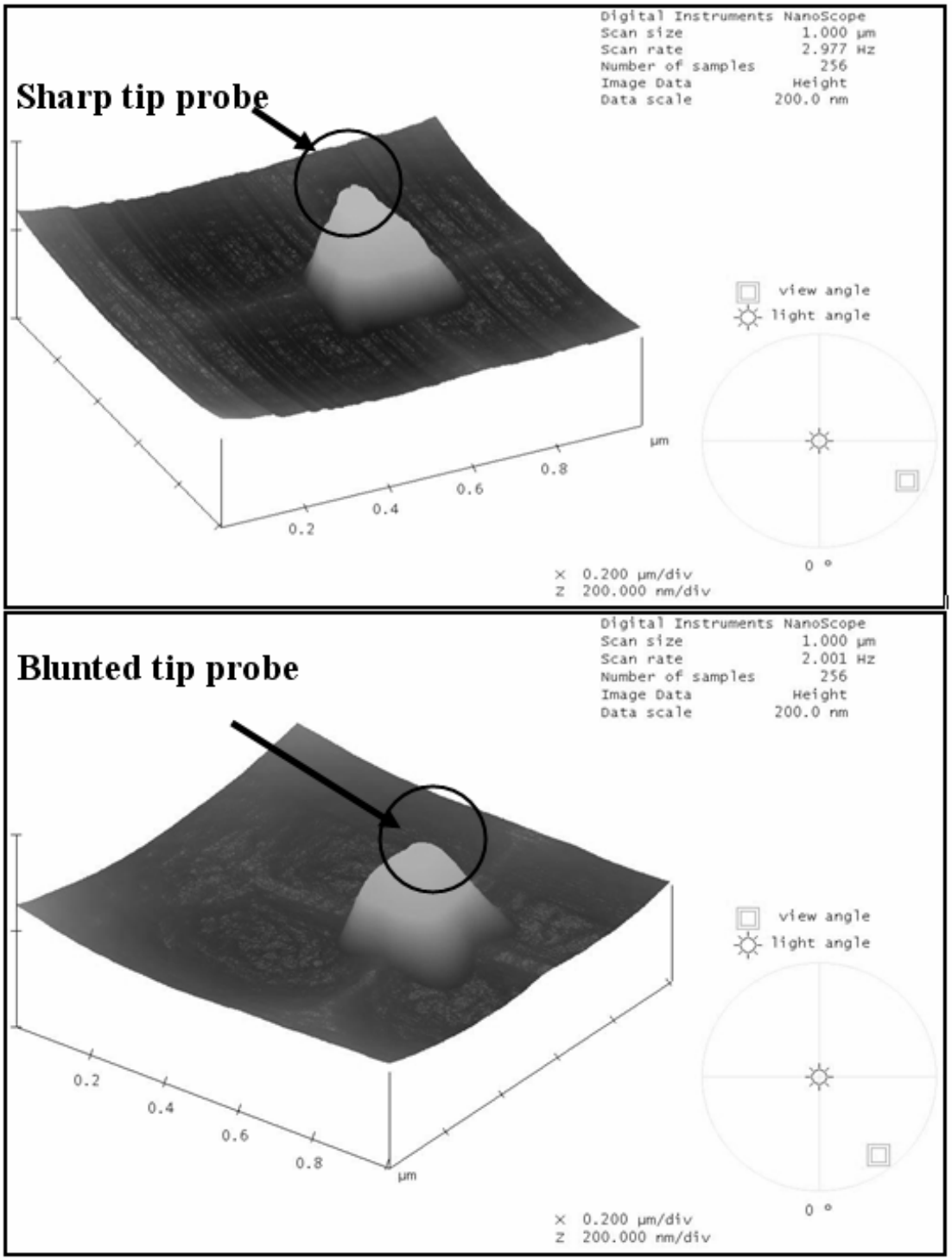
Sharp tip probe
Digital Instruments NanoScope
Scan size 1.000 µm
Scan rate 2.977 Hz
Number of samples 256
Image Data Height
Data scale 200.0 nm
view angle
light angle
µm
0.2
0.4
0.6
0.8
0 °
X 0.200 µm/div
Z 200.000 nm/div
Blunted tip probe
Digital Instruments NanoScope
Scan size 1.000 µm
Scan rate 2.001 Hz
Number of samples 256
Image Data Height
Data scale 200.0 nm
view angle
light angle
0.2
0.4
0.6
0.8
µm
0 °
X 0.200 µm/div
Z 200.000 nm/div

Figure 8.

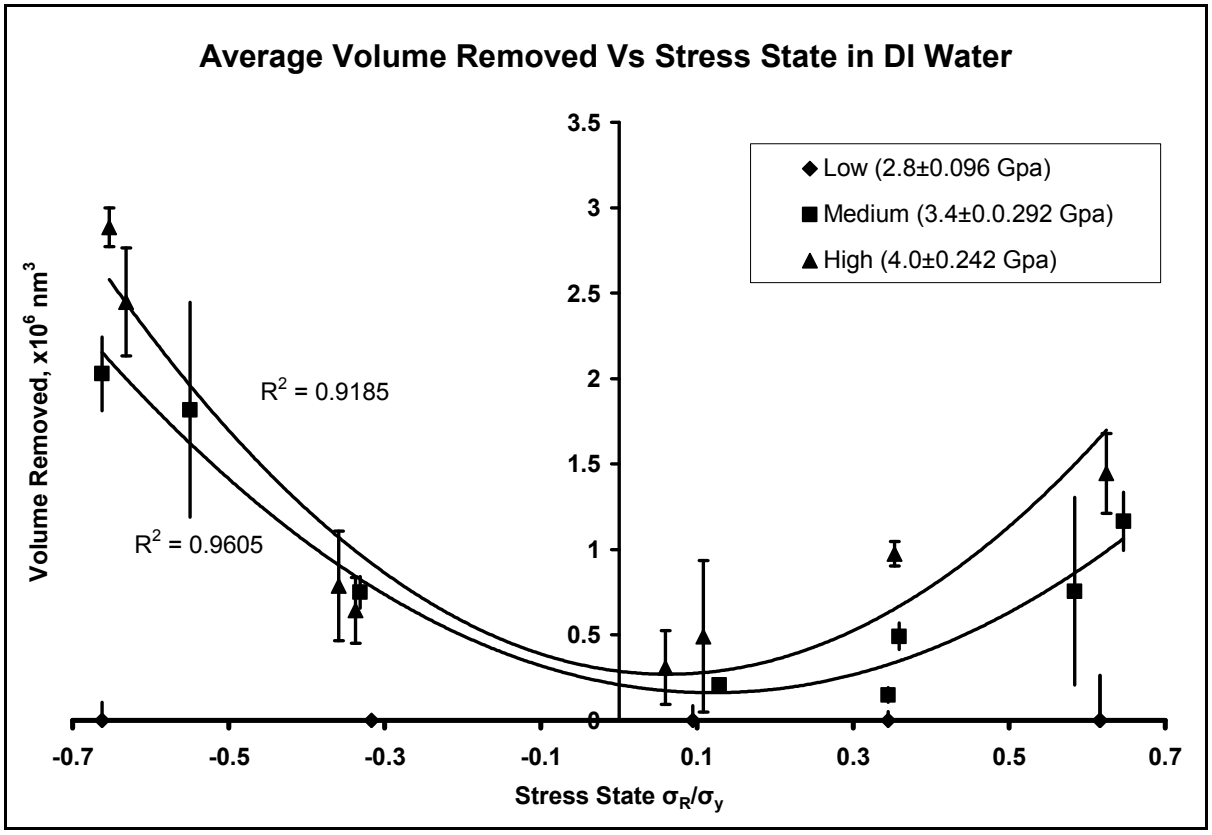
Average Volume Removed Vs Stress State in DI Water
Low (2.8±0.096 Gpa)
Medium (3.4±0.0.292 Gpa)
High (4.0±0.242 Gpa)
R2 = 0.9185
R2 = 0.9605
Volume Removed, x10^6 nm^3
Stress State σR/σy
3.5
3
2.5
2
1.5
1
0.5
0
-0.7
-0.5
-0.3
-0.1
0.1
0.3
0.5
0.7

Figure 9.

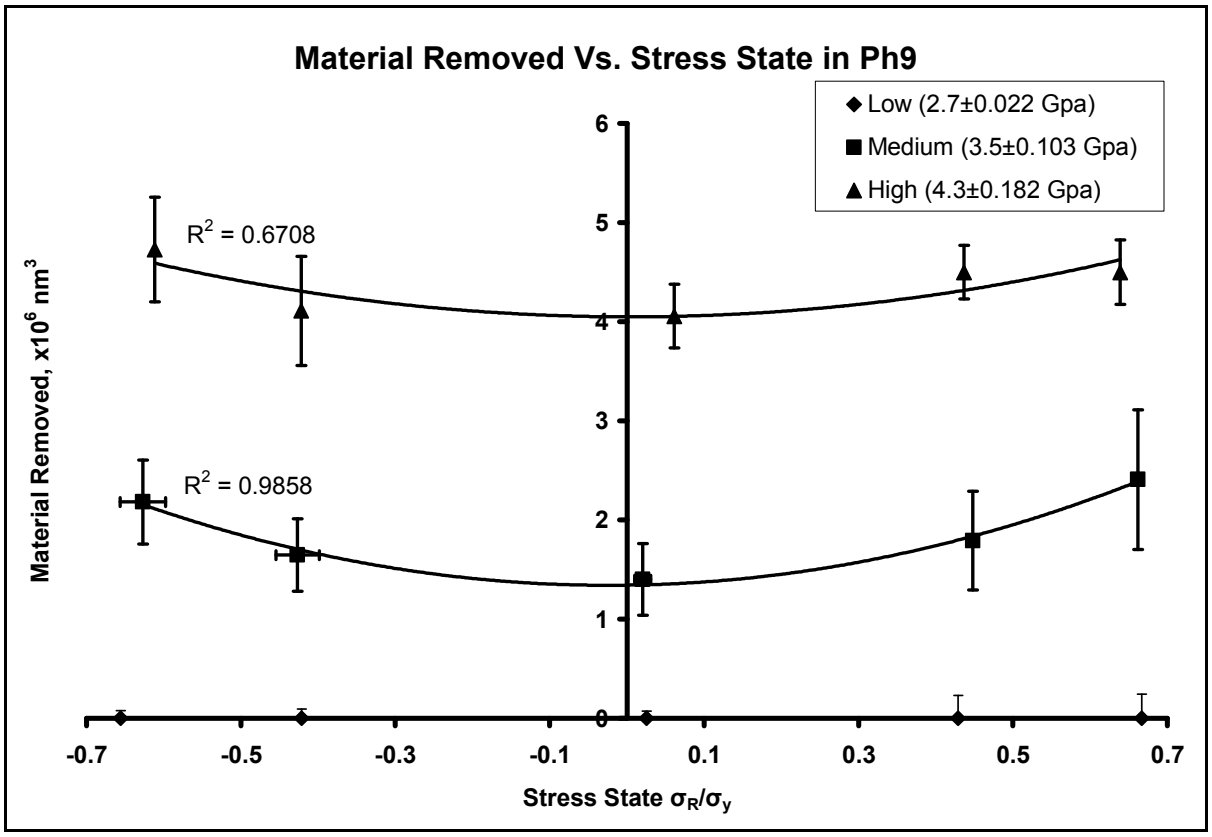
Material Removed Vs. Stress State in Ph9
Low (2.7±0.022 Gpa)
Medium (3.5±0.103 Gpa)
High (4.3±0.182 Gpa)
R2 = 0.6708
R2 = 0.9858
Material Removed, x10^6 nm^3
Stress State σR/σy
6
5
4
3
2
1
0
-0.7
-0.5
-0.3
-0.1
0.1
0.3
0.5
0.7

Figure 10.

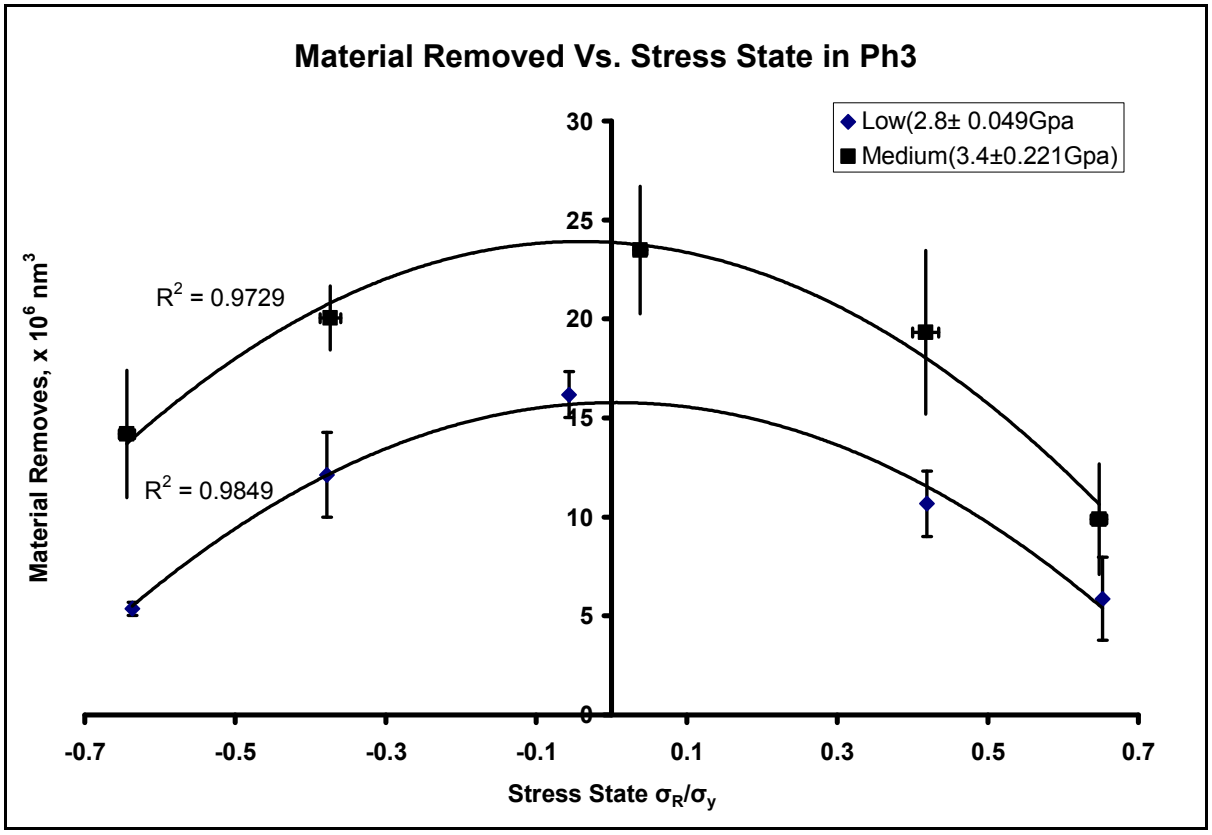
Material Removed Vs. Stress State in Ph3
Low(2.8± 0.049Gpa
Medium(3.4±0.221Gpa)
R2 = 0.9729
R2 = 0.9849
Material Removes, x 10^6 nm^3
Stress State σR/σy
30
25
20
15
10
5
0
-0.7
-0.5
-0.3
-0.1
0.1
0.3
0.5
0.7

Figure 11.

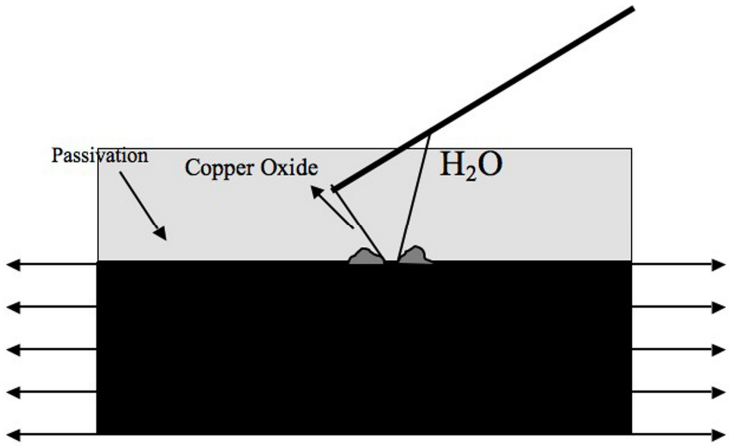

(a)

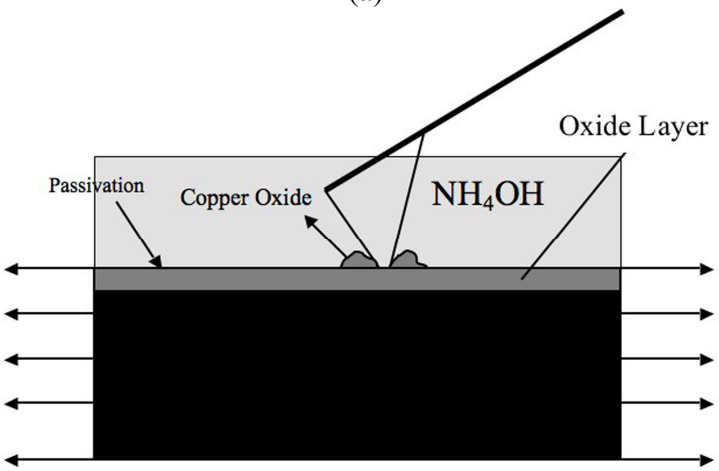

(b)

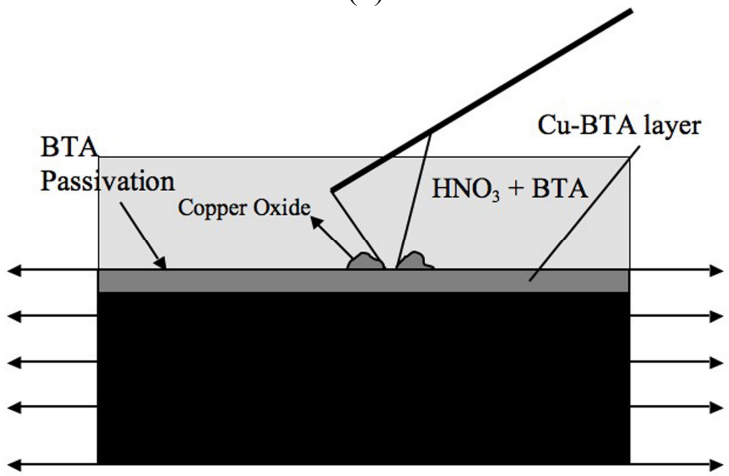

(c)

CHAPTER 5: CONCLUSIONS

5.1 General Discussion and Conclusion

Single asperity wear of copper was investigated as a function of contact pressures, surface stress states and environments. The effect of contact pressures on material removal during wear is significant as expected. High contact pressures accelerate material removal rate. However, it was observed in the results obtained in ambient, slightly acidic and alkaline environments, the material was being removed only the average applied contact pressure exceeds a threshold of 3Gpa. But in acidic condition, the surface damage occurs even with contact pressures less than 3Gpa. When the sample surface is exposed to the acidic environment, it causes the material of the surface is being softened and corroded due to the nature of copper is in corrosion condition for environment with pH of less than 7.

A four-point-bending setup was used to generate a wide range of surface stresses. The setup supplies surface stress varying from compressive to tensile across the sample. The surface stress at a specific location can be determined by knowing the distance of the scan areas away from the neutral axis. The influence of the surface stress state on material removal is more complicated and changes with the chemical environments. In order to better understand the combination effects of surface stress state and chemical environment on material removal rate, it was necessary to perform the experiment in both dry and aqueous conditions. The results will be discussed in the next paragraphs.

In ambient non-reactive condition, a linear distribution of material removal as a function of surface stress state is observed. Material removal is accelerated by the compressive stress while tensile stress suppresses surface damage. The finding is reasonable

since the surface stress is linearly distributed across the sample where the maximum compressive stress at the top of the sample and maximum tensile stress the bottom. However, when the material removal reaches the lowest surface damage at certain tensile stress level, in this case 30% of the copper yield strength, no further damage is observed.

Results obtained in aqueous condition show very different behaviors. In slightly acidic environment (pH6), surface damage follows a skewed quadratic dependence on surface stress state where both compressive and tensile stresses accelerate the material removal. Higher surface damage is observed in the compressive side compared to the tensile side of the sample. This indicates that surface damage proceeds through superposition of two different processes: linear dependence of surface stress as observed in ambient condition and even quadratic dependence of surface stress. In passivating basic environment (pH 9), the surface wear is almost independent of surface stress and only affected by applied contact pressure. In acidic condition, since copper is continuously corroded, a corrosive inhibitor (BTA) was added to form a thin firm (Cu-BTA) on the surface of the sample to serve an oxide layer to prevent material dissolution. Surface is also quadratic influenced by surface stress state but, interestingly, both compressive and tensile stresses suppress the material removal. The chemical passivation process is accelerated and corrosion is suppressed by the surface stress state.

5.2 Significant Findings

The material removal rate of a polishing process is not only affected by contact load and polishing speed. It is also influenced by surface stress state and environment. To the knowledge of the authors, this research is the first to encounter the different surface damage

behaviors effect of surface stress on chemical dissolution and passivation processes. It also verifies the results obtained in the previous works regarding the material removal during a scratching process are influenced by the contact load, surface stress state and environment.

5.3 Future Works

It is the author's hope that this investigation can lead to a better understanding of mechanism of surface delamination and chemical reactions affected by surface stress state and environment. Currently, it is in the preparation stage that similar experiment will be performed on Ti-6Al-4V because of the gaining interest of the material in medical devices. By using the similar approach, it gives better understanding of the wear process and the lifespan of the medical devices can be improved. Since cobalt chromium and copper follow the same trend, the experiment of Ti-6Al-4V performed in ambient condition is expected to follow the similar manner. However, researches have shown different behavior when the materials were exposed to different environment. Therefore, the chemical reaction in the future study is expected to be different and complicated depending on the mechanical loading and environment.